

A multi-model evaluation of aerosols over South Asia: Common problems and possible causes

Xiaohua Pan¹, Mian Chin¹, Ritesh Gautam^{1,2}, Huisheng Bian^{1,3}, Dongchul Kim^{1,2}, Peter R. Colarco¹, Thomas L. Diehl^{1,2,*}, Toshihiko Takemura⁴, Luca Pozzoli⁵, Kostas Tsigaridis^{6,7}, Susanne Bauer^{6,7}, Nicolas Bellouin⁸

1. NASA Goddard Space Flight Center, Greenbelt, MD, United States.

2. Universities Space Research Association, Columbia, MD, United States.

3. University of Maryland Baltimore City, Baltimore, MD, United States.

4. Kyushu University, Fukuoka, Japan.

5. Istanbul Technical University, Istanbul, Turkey.

6. NASA, Goddard Institute for Space Studies, New York, NY, United States.

7. Center for Climate Systems Research, Columbia University, New York, NY, United States.

8. Department of Meteorology, University of Reading, Reading, Berkshire, United Kingdom.

* Current address: European Commission at the Joint Research Center, Ispra, Italy

Correspondence to Xiaohua Pan (xiaohua.pan@nasa.gov)

Abstract

Atmospheric pollution over South Asia attracts special attention due to its effects on regional climate, the water cycle, and human health. These effects are potentially growing owing to rising trends of anthropogenic aerosol emissions found there. In this study, the spatio-temporal aerosol distributions over South Asia from 7 global models, for the period of 2000-2007, are evaluated systematically against aerosol retrievals of NASA satellite sensors and ground-based measurements. Overall, substantial underestimations of aerosol loading over South Asia are found systematically in 6 out of 7 models. Averaged over the entire South Asia, the annual mean Aerosol Optical Depth (AOD) is underestimated by a range of 18%-45% across models compared to MISR, which is the lowest bound among various satellite AOD retrievals (from MISR, SeaWiFS, MODIS Aqua and Terra). In particular at Kanpur located in northern India, AOD is underestimated even more by a factor of 4, and annual mean Aerosol Absorption Optical Depth (AAOD) is underestimated by about a factor of 2 in comparison with AERONET, during the post-monsoon and the wintertime periods (i.e. October-January) when agricultural waste burning and anthropogenic emissions dominate. The largest model underestimation of aerosol loading occurs in the lowest boundary layer (from surface to 2km) based on the comparisons with aerosol extinction vertical distribution from CALIOP. The possible causes for the common problems of model aerosol underestimation over south Asia are identified **in this study**. During the winter, not only the columnar aerosol loading in models, but also surface concentrations of all aerosol components (sulfate, nitrate, organic aerosol and black carbon) are found lower than observations (ISRO-GBP, ICARB and CALIOP), indicating that anthropogenic emissions, especially biofuel, are likely underestimated in this season. Nitrate, a major component of aerosols in South Asia, is either not considered in 4 out of 7 models or

Xiaohua 1/13/2015 3:12 PM

Deleted: SO

Xiaohua 1/13/2015 10:43 AM

Deleted: here, which are suggested as the following

Xiaohua 1/13/2015 3:12 PM

Deleted: SO

47 significantly lower than observations in other 2 models. Surprisingly, the near-surface
48 relative humidity in these models is found significantly lower than observations in the
49 winter, resulting in suppression of the hygroscopic growth of soluble aerosols and
50 formations of sulfate and nitrate, and thereby **low bias** of AOD. During the post-
51 monsoon season, the deficiency of agricultural waste burning emissions in GFED2
52 biomass burning emission inventory, used by the models, partly contributes to the
53 model underestimation of aerosol loading over South Asia in burning seasons.

Xiaohua 1/23/2015 2:35 PM

Deleted: underestimation

54

55 1. Introduction

56 South Asia (Fig.1), particularly the Indo-Gangetic Plain (IGP) in northern India, is one of
57 the global hotspots with high aerosol optical depth (AOD) routinely observed from
58 satellite remote sensing observations (e.g. from Moderate Resolution Imaging
59 Spectroradiometer or MODIS, Multi-angle Imaging SpectroRadiometer or MISR and
60 Sea-Viewing Wide Field-of-View Sensor or SeaWiFS), as well as from ground-based
61 measurements (e.g. Aerosol Robotic Network or AERONET). The potential influence of
62 absorbing aerosols on the climate and water cycle **in this region** (e.g. Indian summer
63 monsoon) via surface dimming and atmospheric warming is widely discussed in the
64 literature (e.g. Ramanathan et al., 2005; Lau et al., 2006). In addition, recent studies
65 have showed that large concentrations of absorbing aerosols, such as dust and black
66 carbon (BC), over the IGP and Himalayan foothills are linked to snow albedo reduction
67 and accelerated snow/ice melt in the Himalaya during the pre-monsoon season (Lau et
68 al., 2010; Qian et al., 2011; Yasunari et al., 2010; Gautam et al., 2013). BC surface
69 concentrations in northern India have been reported to be much higher than in other
70 world regions and mega cities (Tripathi et al., 2005; Ganguly et al., 2006), and the
71 atmospheric heating due to aerosols (mainly BC) is estimated to be large, about 50-70
72 $W m^{-2}$, especially during the wintertime (Ganguly et al., 2006).

Xiaohua 1/13/2015 10:44 AM

Deleted: South Asian

Xiaohua 1/13/2015 10:47 AM

Deleted: also

73 Besides these climate impacts, fine aerosol particles ($PM_{2.5}$ – particulate matter
74 less than 2.5 μm in diameter) are known to affect public health, especially over the IGP
75 region where large portions of the Indian population live. At Delhi, for example, $PM_{2.5}$
76 concentration in 2007 was $97 \pm 56 \mu g/m^3$ (Tiwari et al., 2009), nine times the 2005 air
77 quality guidelines recommended by the World Health Organization. Increases in
78 anthropogenic aerosol emissions and loading in South Asia in recent decades have
79 been well documented (Ohara et al., 2007; Hsu et al., 2012; Kaskaoutis et al. 2012;
80 Babu et al., 2013), contrasting with decreasing trends emissions over Europe and North
81 America (Hsu et al., 2012; Chin et al., 2014).

Xiaohua 1/23/2015 2:32 PM

Deleted: the annual mean

Xiaohua 1/23/2015 2:32 PM

Deleted: about

Xiaohua 1/13/2015 10:49 AM

Deleted: (WHO)

Xiaohua 1/13/2015 10:50 AM

Deleted: -

82 **It is worth to highlight that Kanpur, an urban city in North India, was reported as**
83 **the lowest scoring site next to Beijing out of 21 reprehensive AERONET stations, with overall**
84 **poor event scoring by all four latest generation of quasi-operational aerosol models participating**
85 **in International Cooperative for Aerosol Prediction (ICAP) (Sessions et al. 2015).** The
86 performances of aerosol forecast and future climate projections **as well as the study of**
87 **interaction of aerosol and climate aforementioned** depend on the reliability of the model

Xiaohua 1/13/2015 10:51 AM

Deleted: It is undoubted that the study of interaction of aerosol and climate as mentioned above as well as

98 | simulations of the past and current climate. Therefore, it is critical to accurately
 99 | represent aerosol sources, distributions and properties in climate models over this
 100 | heavily polluted region. Previous studies, however, reported that global models
 101 | underestimated AOD over South Asia, especially over the IGP in the winter (Dickerson
 102 | et al., 2002; Reddy et al., 2004; Chin et al., 2009; Ganguly et al., 2009; Henriksson et al.,
 103 | 2011; Goto et al., 2011; Cherian et al., 2013; Sanap et al., 2014). Among them, Ganguly
 104 | et al. (2009) reported that the GFDL-AM2 model largely underestimated the AOD over
 105 | the IGP during the winter by about a factor of 6. Recently, AOD simulated by the
 106 | regional climate model (RegCM4) showed a good agreement with the observed AOD
 107 | from AERONET over dust-dominated areas in south Asia, but AOD was underestimated
 108 | over regions that are dominated by anthropogenic emission (Nair et al., 2012). Eleven
 109 | of the twelve models participating in the AeroCom phase I model intercomparison were
 110 | also found to underestimate the aerosol extinction over South Asia, especially under 2
 111 | km, in comparison with the space-borne lidar measurements from the Cloud–Aerosol
 112 | Lidar and Infrared Pathfinder Satellite Observations (CALIPSO) satellite (Koffi et al.,
 113 | 2012). The ability to capture surface BC concentrations over South Asia for models has
 114 | been found limited. The low biases tend to be larger in the winter (Ganguly et al., 2009;
 115 | Menon et al., 2010; Nair et al., 2012; Moorthy et al., 2013). These studies have revealed
 116 | the challenges for models to adequately represent the aerosol loading.

117 | Extending from previous studies and utilizing the recent model outputs from the
 118 | Aerosol Comparisons between Observations and Models (AeroCom) Phase II multi-
 119 | model experiments, the present work systematically evaluates global model simulations
 120 | of aerosols in South Asia with observations from satellites and ground-based
 121 | measurements, and strives to characterize the causes for the model deficiency in
 122 | reproducing observations. The outcomes of this study will help us understand the
 123 | discrepancies between models and observations, thus providing directions for future
 124 | model improvements in this important region.

125 | The description of models is given in section 2. The observation data from
 126 | satellites and ground-based measurements are introduced in section 3. We present the
 127 | results in section 4, including the comparisons of the multi-model simulations with
 128 | observations in terms of horizontal, vertical and temporal distribution of AOD (and
 129 | aerosol absorption optical depth, or AAOD when available), and the surface BC
 130 | concentration. The possible causes for the underestimations of aerosol load found in
 131 | models are investigated in section 5. Major findings are summarized in section 6.

132 | 2. Model description

133 | 2.1 Models

134 | The aerosol simulations for the period of 2000-2007 from 7 models, including 6 models
 135 | that participated in AeroCom Phase II hindcast experiment (i.e. AeroCom II HCA) and
 136 | one additional model, GEOS5, are analyzed in this paper (see Table 1 for details).
 137 |

Xiaohua 1/13/2015 10:52 AM

Deleted: , South Asia

Xiaohua 1/13/2015 10:52 AM

Deleted: the

Xiaohua 1/23/2015 2:40 PM

Deleted: the

Xiaohua 1/13/2015 10:53 AM

Deleted: impacted

Xiaohua 1/13/2015 10:54 AM

Deleted: In terms of aerosol vertical
distribution over South Asia,

Xiaohua 1/13/2015 10:54 AM

Deleted: 11

Xiaohua 1/13/2015 10:54 AM

Deleted: 12

Xiaohua 1/13/2015 10:55 AM

Deleted: vertical

Xiaohua 1/14/2015 1:37 PM

Deleted: (Yu et al., 2010;

Xiaohua 1/13/2015 10:56 AM

Deleted: similarly

Xiaohua 1/13/2015 12:54 PM

Deleted: over South Asia

Xiaohua 1/14/2015 2:56 PM

Formatted: Font:11 pt

Xiaohua 1/23/2015 2:41 PM

Deleted: of South Asia

151 Given that MODIS-Terra is available only after 2000, we chose the years 2000-2007 in
 152 this study, although longer time period of simulations (starting from 1980) are available
 153 from six AeroCom models (note that ECHAM5-HAMMOZ ended in 2005 and HadGEM2
 154 in 2006). GEOS5 is similar to GOCART because its aerosol module is developed from
 155 GOCART but with modifications (Colarco et al., 2010). More detailed descriptions about
 156 these models can be found in previous studies (see references listed in Table 1 and
 157 Myhre et al., 2013). All models include sulfate (SO_4^{2-}), BC, organic aerosol (OA), dust
 158 (DU) and sea salt (SS). Nitrate (NO_3^-) is included in only three models (GISS-modelE,
 159 GISS-MATRIX and HadGEM2). The secondary organic aerosol (SOA) chemistry is
 160 resolved only in two models, GISS-modelE and HadGEM2 (offline scheme in this
 161 model), and simple estimations of SOA are included in the remaining models. Among
 162 seven models, aerosol optical properties are treated differently although all optical
 163 properties are derived from Mie theory. In order to compare closely with the
 164 measurements from satellites and AERONET that are under clear-sky conditions, clear-
 165 sky AODs of the two GISS models are used in this study, which is not available in other
 166 5 models (only all-sky AOD is available). In general, clear-sky AOD is lower than its
 167 corresponding all-sky AOD (e.g. by 60% based on GISS-modelE at Kanpur). All 7
 168 models use the assimilated wind fields, although from different assimilation datasets.
 169 The horizontal resolutions vary from 2.8° by 2.8° (ECHAM5-HAMMOZ) to about 1.1° by
 170 1.1° (SPRINTARS) and the vertical levels range from 30 (GOCART-v4) to 72 (GEOS5).
 171 More information is given in Table 1.

173 2.2 Emissions

174 For anthropogenic emissions, which are mainly from consumption of fossil fuel and
 175 biofuel, the models choose either A2-ACCMIP or A2-MAP emission dataset. Both A2-MAP
 176 and A2-ACCMIP were constructed by combining multiple inventories but in different
 177 ways. The anthropogenic emissions from A2-MAP have inter-annual variability based
 178 on reported activity data, while those from A2-ACCMIP do not because they are
 179 generated via linear interpolation between decadal endpoints. Over South Asia, the
 180 spatial distribution and total emission amount are different between these two emission
 181 datasets, with higher emission amount in A2-ACCMIP. Detailed information on these two
 182 emission datasets can be found in Diehl et al. (2012).

183 Figure 2 shows the averaged annual mean (2000-2007) anthropogenic BC, OA,
 184 SO_2 , NH_3 and NO_x emissions from A2-ACCMIP anthropogenic emission dataset (A2-
 185 MAP is not shown and it does not provide NH_3 and NO_x emissions). Note that the
 186 seasonal cycle of anthropogenic emission is not resolved in either emission dataset,
 187 which could be problematic especially for biofuel emission in this region (discussed in
 188 Section 5.3). The anthropogenic emissions display high spatial heterogeneities over
 189 South Asia, coinciding with those of the population distribution as reported by multiple
 190 previous studies (e.g. Girolamo et al., 2004). Densely populated regions are usually

Xiaohua 1/23/2015 2:42 PM

Deleted: the

Xiaohua 1/23/2015 2:43 PM

Deleted: 3

Xiaohua 1/23/2015 2:43 PM

Deleted: 2

Xiaohua 1/13/2015 12:55 PM

Deleted: i.e.

Xiaohua 1/23/2015 2:43 PM

Deleted: the 7

Xiaohua 1/14/2015 1:38 PM

Deleted: the models choose one of two emission datasets: A2-ACCMIP or A2-MAP

Xiaohua 1/14/2015 1:31 PM

Deleted: 2

200 associated with heavy anthropogenic emissions in south Asia, especially the IGP region
 201 in northern India (as indicated in Fig. 1). In A2-ACCMIP (A2-MAP), the annual mean
 202 anthropogenic aerosols emissions in South Asia for 2000-2007 are 7.426 (5.279) Tg
 203 $\text{SO}_2 \text{ yr}^{-1}$, 4.934 Tg $\text{NH}_3 \text{ yr}^{-1}$, 4.330 Tg $\text{NO}_x \text{ yr}^{-1}$, 3.455 (2.678) Tg C yr^{-1} of organic aerosol
 204 (OA), and 0.681 (0.633) Tg C yr^{-1} of BC, (refer to Fig. 2 for the spatial distribution of
 205 these anthropogenic emissions).

206 Open biomass burning, including the agricultural residue burned in the field and
 207 forest burning, also contribute significantly to the total aerosol loading over India, about
 208 25% of BC and OC (Venkataraman et al., 2006). Figure 3 shows the seasonal BC
 209 biomass burning emission based on monthly Global Fire Emissions Database Version 2
 210 (GFED2), from which the biomass burning emissions in A2-ACCMIP and A2-MAP
 211 emissions inventories are derived. OA and SO_2 show similar spatial patterns and
 212 proportional amounts as BC (not shown here). The open biomass burning displays
 213 strong geographical and seasonal variations. Pre-monsoon period is the most active
 214 open biomass burning season with an emission amount of 0.118 Tg C yr^{-1} over South
 215 Asia, especially concentrated over northeastern India associated with the Jhum
 216 cultivation to clear the forest and create fields (Vadrevu et al., 2013). Seasonal practices
 217 of biomass burning from agricultural crop residues associated with rice-wheat crop
 218 rotation system over the western IGP, such as Punjab, Haryana and western Uttar
 219 Pradesh, could explain the high aerosol loading during the post-monsoon season
 220 (Badarinath et al., 2009a; Sharma et al., 2010; Vadrevu et al., 2011; Vadrevu et al.,
 221 2013) with a total emission amount of 0.011 Tg C yr^{-1} over South Asia.

222 The major natural aerosol over South Asia is the wind-blown mineral dust from
 223 the arid and semi-arid regions of southwest Asia, such as Iran, Afghanistan, Pakistan,
 224 Arabian Peninsula, and Thar Desert in the northwestern India. The dust emissions
 225 among the model simulations are quite diverse, which vary from 11.7 ± 4.2 (ECH) to
 226 157.4 ± 28.8 (SPR) Tg yr^{-1} (averaged for 2000-2007 over South Asia). This model
 227 diversity is attributed to differences in the model size range of the emitted particles,
 228 parameterization of source strength, and wind fields and soil properties over source
 229 regions. Since this specified region mainly consists of land areas, the sea salt emission
 230 is negligible.

231

232 3. Observation dataset

233 3.1 Satellite data

234 In this study, five satellite data products are used to characterize aerosol distribution
 235 and evaluate the model simulations. Level 3 monthly AOD from MODIS Terra and Aqua
 236 Collection 5.1 were produced by averaging the daily aerosol products at $1^\circ \times 1^\circ$ grid. The
 237 MODIS AOD (at 550 nm), shown in this study, is a composite of the Dark Target (Levy
 238 et al., 2010) and Deep Blue retrieval products (Hsu et al., 2006), as the latter is able to
 239 retrieve AOD over bright surfaces such as the Thar Desert. The SeaWiFS aerosol

Xiaohua 1/13/2015 2:38 PM
Deleted: such as

Xiaohua 1/13/2015 2:42 PM
Deleted: from SO_2

Xiaohua 1/13/2015 2:43 PM
Deleted: is

Xiaohua 1/13/2015 2:38 PM
Deleted: about

Xiaohua 1/13/2015 2:42 PM
Deleted: , NH_3 about

Xiaohua 1/13/2015 2:45 PM
Deleted: 4

Xiaohua 1/13/2015 2:43 PM
Deleted: NO_x is about

Xiaohua 1/13/2015 2:43 PM
Deleted: , Organic aerosol (OA) about

Xiaohua 1/13/2015 2:43 PM
Deleted: ,

Xiaohua 1/13/2015 2:44 PM
Deleted: BC about

Xiaohua 1/13/2015 2:48 PM
Deleted: in South Asia

Xiaohua 1/13/2015 2:52 PM
Deleted: the entire

retrieval combined the Deep Blue algorithm over land (Hsu et al., 2006, 2012) and Ocean Aerosol Retrieval (SOAR) algorithm over ocean (Sayer et al., 2012). MISR (at 555 nm) retrieves aerosol properties over a variety of terrain, including bright surface like deserts, which is attributed to its unique multi-angle capability (Martonchik et al., 2004; Kahn et al., 2007). Since South Asia is covered by frequent cloudiness during the summer monsoon season (June to September), the quality of monthly mean AOD during this season is likely to be affected by the low sample size.

The retrieval uncertainties and error estimates of the satellite products we used in this study have been published extensively, including addressing the impact of errors in the surface reflectance on aerosol retrieval qualities (e.g., Levy et al., 2007, 2010; Kahn et al., 2007, 2010; Sayer et al., 2012, 2013; Hsu et al., 2006). These aerosol products (from MODIS, MISR and SeaWiFS) are regionally validated retrievals with reference to AERONET sites located worldwide, and include uncertainties (e.g. due to surface reflectance) as part of each product's accuracy assessment. For example, MODIS dark-target aerosol product has an improved surface reflectance parameterization introduced in collection 5.1 AOD dataset (Levy et al. 2007), which is used in our paper, with its overall uncertainty over land reported to be within $\pm(0.05\pm0.15\%)$ AOD and better for oceanic regions (Levy et al., 2010). Whereas, about 70% of the MODIS Deep Blue (aerosol retrievals over bright reflecting surfaces such as desert/arid regions) and SeaWiFS AOD (over both bright desert/arid regions and vegetated surface) retrievals fall within an expected absolute uncertainty of $0.05 \pm 20\%$ (for the wavelength of 550nm AOD used in our paper) (Sayer et al. 2012, 2013). It should also be noted that only the best-quality aerosol retrievals are aggregated to form the Level-3 gridded monthly mean AOD dataset, which is being used in our paper. Similarly, aerosol retrievals from MISR have comparable or better accuracy assessment as part of their overall uncertainty (Kahn et al. 2010).

The monthly mean AOD and vertical extinction from several satellite products (MODIS, MISR, SeaWiFS, and CALIOP) are used to compare with the models. Although the satellite data are averaged over the "snap shot" observations at the local overpassing time (varying between 10:30AM to 1:30PM) and the model results are diurnally averaged, previous studies compared model simulated AOD sampled at MODIS/MISR overpass times with that averaged over diurnal time steps and found the differences were small on monthly mean AOD, only about 10% in south America and southern Africa (i.e. biomass burning regions) and smaller elsewhere (Colarco et al., 2010). Thus, the bias caused by time difference is expected to be small in our study, since we are using monthly mean satellite data products in comparison to monthly mean model AOD simulations.

The vertical extinction profiles from the Cloud-Aerosol Lidar with Orthogonal Polarization (CALIOP) onboard the satellite CALIPSO layer product version 3.01 (climatology of June 2006-December 2011) are used to evaluate the model simulated aerosol vertical distribution in 2006 (CALIPSO 2011; Koffi et al., 2012). Only the CALIOP observations in 532 nm channel and nighttime are used because of their better signal-to-noise than the 1064 nm and daytime observations. Three parameters are applied to facilitate this evaluation, namely AOD, Z_a (km) and F_{2km} (%). AOD is the integral of extinction coefficient within the entire column (Eq. 1). Z_a is defined as the averaged aerosol layer height (Eq. 2). F_{2km} is defined as the percentage of AOD located in the lowest 2 km (Eq. 3) in the column.

$$AOD = \sum_{i=1}^n EXT_i \times \Delta Z_i \quad (1)$$

$$Z_a = \frac{\sum_{i=1}^n EXT_i \times Z_i}{\sum_{i=1}^n EXT_i} \quad (2)$$

$$F_{2km} = \frac{\sum_{i=1}^{level\ of\ 2km} EXT_i \times \Delta Z_i}{\sum_{i=1}^n EXT_i \times \Delta Z_i} \quad (3)$$

Where, EXT_i is the extinction coefficient at i level ($i=1$ to n , i.e. from the lowest 100m to the top of atmosphere), Z_i is altitude (km) of level i and ΔZ_i is the depth of level i .

3.2 AERONET

In this study, we use AOD and AAOD data from the ground-based AERONET (Holben et al., 1998) sites in South Asia. Monthly mean AOD and AAOD at 500nm were analyzed over Kanpur, Lahore and Karachi. Here, version 2 Level-2 data were used, which are cloud-screened and quality-assured. Locations of these three stations are shown in Fig. 1 along with 11 in-situ measurement sites as described in the following Section 3.3. The information of all 14 ground-based measurement sites is given in Table 2.

3.3 In-situ measurements

We evaluate the modeled BC concentrations with the surface in-situ measurements from the Integrated Campaign for Aerosols gases and Radiation Budget (ICARB) field campaign in India over 8 stations, which spread over Indian mainland and islands for the entire year of 2006. The measured ICARB BC data is recorded from inter-compared aethalometers following a common protocol. More details of ICARB can be found in previous publications (e.g. Beegum et al., 2009 and Moorthy et al., 2013).

In order to examine the chemical composition (such as surface concentrations of nitrate, sulfate, organic aerosol and black carbon) and meteorological conditions (such as surface relative humidity and temperature) of winter haze over IGP in multi-models, we refer to the measurements from the Indian Space Research Organization

Xiaohua 1/23/2015 2:54 PM

We also use

Xiaohua 1/23/2015 2:54 PM

t

Xiaohua 1/14/2015 1:41 PM

Xiaohua 1/14/2015 1:41 PM

α

Geosphere Biosphere Programme (ISRO-GBP) which provided valuable information about aerosol physical, optical and chemical properties along the IGP during wintertime (i.e. December 2004/January 2005). In this study, 4 stations in IGP are selected because of their relatively complete measurements, i.e. Hisar (Ramachandran et al., 2006; Rengarajan et al., 2007; Das et al., 2008), Agra (Safai et al., 2008), Kanpur (Tripathi et al., 2006; Tare et al., 2006) and Allahabad (Ram et al., 2012).

4. Results

In this section, the aerosol simulations by multi-models are evaluated in comparison to satellite data and ground-based measurements in terms of temporal variation and spatial distribution (horizontally and vertically) over South Asia.

4.1 Interannual variability of AOD

Figure 4a shows the annual averaged mean AOD over the entire South Asia domain (denoted by green shaded area) for the period of 2000-2007. The AOD is 0.281 and 0.282 from MISR and SeaWiFS (SeaW) retrievals respectively, and 0.348 and 0.355 from MODIS Aqua (MODIS-a) and Terra (MODIS-t) respectively. Six out of seven models (except for HAD) consistently underestimated AOD by 0.052-0.126 or 18%-45%, compared to MISR, the lowest bound of four satellite retrievals. As shown in Fig. 4b, over the central IGP region (77-83°E/25-28°N, denoted by the white box in Fig. 4a) where the hotspot of AOD is observed from satellites, the performance of the same six models are even worse, with the annual averaged mean AOD underestimated by 20-56% relative to MISR. Unlike other models, HAD shows a comparable AOD with MISR and SeaWiFS over the entire South Asia, and exceeds all satellite data over the central IGP. As shown in Figure 4a, the peak AOD in 2003 and the low AOD in 2005 are reflected in all satellites (except MODIS Aqua), which are positively related to the strength of dust emissions during the dry season in that corresponding year (Kaskaoutis et al., 2012; Hsu et al., 2012; Ramachandran et al., 2013). However, all models fail to capture these observed interannual variations of AOD, and only two models (GE5 and SPR) indicate the low AOD in 2005.

4.2 Seasonal cycle of AOD and AAOD over 3 AERONET stations

To further examine the details of underestimations occurring in most models, in this section, monthly variations of AOD and AAOD are compared with the AERONET data at three selected sites in South Asia (Fig. 5). These three locations represent different aerosol environments in South Asia: Kanpur, an industrial city located in the central IGP, is influenced by high anthropogenic emissions throughout the year and by the transported dust during pre-monsoon (MAM) and early monsoon periods (JJA); Lahore, located in the western IGP, is directly influenced by the biomass burning in the pre-monsoon (MAM) and post-monsoon (ON) seasons; and Karachi, an urban coastal city in Pakistan, is influenced by the frequent dust outbreaks, especially from the Arabian

375 peninsula around early summer monsoon season (JJA). A two-year period is chosen for
376 each site, based on the availability of AERONET measurements at that site. The
377 satellite data, namely MODIS-Terra, MISR, and SeaWiFS, are also shown along with
378 AERONET to make an inter-comparison.

379 At Kanpur (first row of Fig. 5), strong seasonal distribution of AERONET AOD
380 (left column of Fig. 5) are associated with dust outbreaks in May-July, and the active
381 open biomass burning as well as high anthropogenic emissions in October-January.
382 However, only the peak in May-July each year is captured by most models (except
383 HAD) although overestimated in GIM, while the other peak in October-January is largely
384 missing in all models. Different from observations and other models, HAD model
385 simulates AOD with two peaks in April and October, out-of-phase with the observed
386 seasonal cycles. The observed and modeled features mentioned above are repeated
387 almost every year. The discrepancy among models and from AERONET AOD is further
388 diagnosed in the end of this section. As for AAOD (right column of Fig. 5), all models
389 are much lower than the AERONET retrieval by a factor of 2 on average. Although 2
390 out of 7 models show enhanced AAOD during the dusty period, large underestimation
391 are still pronounced in other models and other seasons when anthropogenic/open
392 biomass burning emissions dominate, implying the underestimation of BC loading or
393 misrepresentation of its optical properties (more analysis on BC in Section 4.5).

394 At Lahore (second row of Fig. 5), AERONET data is available mostly in 2007,
395 when model outputs are available only from five models. Lahore is located in the Punjab
396 region, which is an agriculture region known as the “breadbasket” for the Pakistan and
397 India. The enhanced AERONET AOD and AAOD are evident at Lahore during October-
398 November as shown in Fig. 5, which is linked to the agricultural waste burning after
399 harvest in this area. However, all five models underestimate AOD in each single month,
400 with the largest underestimation found in the October-November (similarly for AAOD).
401 Thereby it suggests that emissions from agriculture waste burning, which is based on
402 GFED2, are likely underestimated in these models (discussed in Section 5.4).
403 Compared to observations, HAD again showed abnormal seasonal variation at Lahore
404 as at Kanpur with extreme high AOD in October.

405 At Karachi (third row of Fig. 5) in 2007, an unimodal distribution is revealed in
406 AERONET AOD, in contrast to the bimodal seasonal variation at Kanpur. The maximum
407 AOD around July is associated with the wind-driven mineral dust from the Arabian
408 Peninsula, which is captured by the models. However, similar to Lahore, all models fail
409 to capture the relative higher AAOD around November, when the open biomass burning
410 is active in the northwestern South Asia (i.e. the area around Lahore) and the smoke is
411 transported southward to the region where Karachi is located (Badarinath et al.,
412 2009a,b).

413 Overall, in comparison with AERONET and satellite data at the three stations,
414 most models tend to underestimate AOD in October-January when the open biomass

Xiaohua 1/14/2015 1:31 PM
Deleted: 3

416 burning and anthropogenic emissions are dominant over dust emissions. Regarding the
417 comparison between satellite and AERONET AOD data at these three stations, the
418 monthly variations and magnitudes of all three satellites generally resemble those of
419 AERONET AOD. However, MODIS-Terra is biased high during the pre-monsoon and
420 monsoon months. It is partially because the dark target retrieval in MODIS, which is
421 applied over area like Kanpur, is sensitive to the surface reflectance. The surface
422 reflectance is usually biased low under dusty condition (Jethva et al., 2009), and in turn,
423 the atmospheric contribution, i.e. AOD, is biased high.

424 In order to diagnose the discrepancies between models and AERONET data, the
425 individual component AOD from only 4 models (HAD, GE5, SPR and GOC, unavailable
426 from other 3 models) are also examined at Kanpur for 2004 in Fig. 6. It is found that the
427 abnormal high peaks in April and October in the HAD model (upper left panel in Fig. 6)
428 are mainly contributed by the nitrate (NO_3^-) AOD, indicating a problem with simulating
429 the seasonal variation and amount of the nitrate aerosol in this model. On the other
430 hand, in December and January, HAD is the only model with the AOD closest to the
431 AERONET data at Kanpur, largely due to nitrate. In fact, nitrate aerosol is expected to
432 be the highest in winter, because high relative humidity and low temperature over IGP in
433 this season favor the formation of NH_4NO_3 (Lewandowska et al., 2004). However, other
434 three models (SPR, GE5 and GOC) do not have the nitrate aerosol component, which
435 may partially explain the underestimations of the peak in the winter (December and
436 January) in these models. In general, based on the results of column AOD from all
437 these four models (i.e. HAD, GE5, SPR and GOC), it is found that the magnitudes and
438 seasonal cycles of aerosol composition are very different across models, in particular
439 for nitrate, sulfate and dust.

440 4.3 Spatial distribution of AOD in different seasons

442 In the previous section, the underestimations of AOD and AAOD are mainly found in
443 October-January based on the model evaluations at three AERONET stations. Here, as
444 shown in Fig. 7a-b, the spatial distributions of AOD over the entire South Asia are
445 compared among 4 satellites, i.e. MODIS-Terra and MODIS-Aqua at 550 nm, MISR at
446 555 nm and SeaWiFS at 550nm, and 7 models at 550 nm during the winter monsoon
447 (DJF), pre-monsoon (MAM), summer monsoon (JJAS) and post monsoon (ON) phases
448 averaged over 2000-2007. Three aforementioned AERONET stations are also labeled
449 in the spatial maps for reference. In general, the spatial distribution of aerosol is closely
450 associated with the emission source over South Asia, and the aerosol abundance in the
451 atmosphere is modulated by meteorological conditions, such as efficient atmospheric
452 dispersion associated with the prevailing winds in March-July, high wet removal
453 associated with the monsoon rainfall in June–September, and stable atmospheric
454 conditions and thus less efficient atmospheric dispersion in December-February.

Xiaohua 1/23/2015 3:06 PM

Deleted: amplitude

Xiaohua 1/13/2015 5:26 PM

Deleted: Fig. 7

Xiaohua 1/13/2015 5:26 PM

Deleted: d

Xiaohua 1/23/2015 2:59 PM

Deleted: 3

Xiaohua 1/23/2015 3:00 PM

Deleted: at 550 nm

Xiaohua 1/23/2015 3:00 PM

Deleted: (

Xiaohua 1/23/2015 3:00 PM

Deleted: resembles MODIS-Terra)

During the winter season (DJF), local anthropogenic sources dominate over dust, contributing as much as 80% ($\pm 10\%$) to the aerosol loading (Ramanathan et al., 2001). The maximum AOD is found in the central and eastern IGP based on three satellites as shown in Fig. 7a, which coincides with the large SO₂ emissions there (Fig. 2) associated with large thermal power plants (capacity >1970 MW) (Prasad et al., 2006). The natural topography (i.e. gradually decreased elevation eastward but narrow opening to the Bay of Bengal as shown in Fig. 1) is favorable to the accumulation of aerosol over central and eastern IGP. Additionally, the winter season is characterized by relatively stable atmospheric condition that traps pollutants in the shallow **atmospheric** boundary layer (**ABL**), leading to a strengthened hazy condition in the IGP (Girolamo et al., 2004; Gautam et al., 2007). The outflow of aerosols to the Bay of Bengal is well depicted by satellite data. **As shown in the first column of Fig. 7b, however, only the HAD model captures the observed AOD spatial pattern and magnitude.** Other models greatly underestimate the high AOD over IGP region. In addition, the observed north-south gradient of AOD is not captured by most models, with SPR showing no gradient and ECH and GIM showing opposite gradient. The common underestimation over the Indian subcontinent is probably owing to missing aerosol species such as nitrate aerosol (Fig. 6), incorrect meteorological fields such as air temperature and relative humidity, or the underestimation of anthropogenic emissions in these models (discussed in **more** details in Section 5).

Starting from the pre-monsoon season (MAM), the entire South Asia is characterized by high AOD mainly due to the mineral dust transported from the arid and desert region by westerly winds, with maximum AOD over the IGP region seen from three satellites (Fig. 7a). It was reported that dust contributes to 62% of the AOD at Kanpur (Srivastava et al., 2012a). **As shown in the second column of Fig. 7b, however, five models (GE5, GIE, GIM, GOC and SPR) partially capture this spatial distribution.** It is interesting that the model HAD shows high AOD over the northern India, which is dominated by nitrate rather than dust (refer to Fig. 6). The dust source in the northwestern parts of South Asia is missing in HAD as shown in Fig. 7b. The model ECH shows very low AOD and little dust over IGP. Despite these deficiencies, model simulations over South Asia **are closer to the satellite data during the pre-monsoon season** than those during the winter, with the model-averaged AOD capturing **71%** of the **satellite data** in the pre-monsoon season compared to only 54% in the winter.

During the monsoon season (JJAS), the dust transported mainly from the Arabian Peninsula by the strong southwesterly wind explains the high AOD over northwestern India (Fig. 7a). High AOD over the Arabian Sea and southwest Asia is evident from MODIS and MISR. **As shown in the third column of Fig. 7b, most models reproduce both the spatial distribution and the magnitude of AOD during this season,** indicating that these models have captured dust emission over the Arabian Peninsula and its transport to South Asia. However, it should be noted that during the monsoon

Xiaohua 1/13/2015 5:27 PM

Deleted: However,

Xiaohua 1/23/2015 3:06 PM

Deleted: amplitude

Xiaohua 1/13/2015 5:29 PM

Deleted: b

Xiaohua 1/13/2015 5:29 PM

Deleted: F

Xiaohua 1/13/2015 2:57 PM

Deleted: during the pre-monsoon season

Xiaohua 1/13/2015 2:56 PM

Deleted: ed

Xiaohua 1/13/2015 2:56 PM

Deleted: about

Xiaohua 1/13/2015 2:58 PM

Deleted: retrieved ones

Xiaohua 1/13/2015 5:30 PM

Deleted: c

Xiaohua 1/13/2015 5:30 PM

Deleted: M

Xiaohua 1/23/2015 3:06 PM

Deleted: amplitude

season the monthly mean AOD from satellites is likely to be biased high because only limited number of cloud-free days are available for aerosol retrievals (Ramachandran and Cherian, 2008).

During the post-monsoon season (ON) the southwesterly wind significantly weakens, and thus dust transport to the Indian subcontinent is lower compared to the pre-monsoon and monsoon seasons. Based on the spatial distributions from the three satellites (Fig. 7a), high AOD is located over the IGP with maxima over western IGP associated with the biomass burning from the agriculture waste fires particularly in this season (Fig. 3). The burning area is mainly located in the northwestern IGP region, such as Punjab, Haryana and western Uttar Pradesh. With the aid of northwesterly winds, aerosols are transported to the central IGP along the valley as well as southward (Badarinath et al., 2009a, b). As shown in the fourth column of Fig. 7b, however, none of the models capture these features, indicating the biomass burning emissions are severely underestimated in the current inventory based on GFED2, which will be discussed in Section 5.4. In contrast to the underestimations by other models, HAD overestimated AOD over IGP due to the high amount of nitrate (Fig. 6).

4.4 Aerosol vertical distribution

Figure 8 shows the comparison of aerosol extinction profile at 550 nm among models and the CALIOPSO data at 532nm (namely CALIOP) in 4 seasons. In order to show latitudinal gradient, two representative stations are chosen, with Kanpur in northern India and Hyderabad in central India (Fig. 1). Based on CALIOP data at Kanpur ($2^{\circ} \times 2^{\circ}$ box averaged around the station location) in Fig. 8a, the extinction coefficient reaches the maximum value of 0.4 km^{-1} during the winter at $Z_a = 1.18 \text{ km}$, but decreases rapidly upward and diminishes around 4 km. Note that low near-surface values within 180 meters in CALIOP profile is contaminated by the surface return (CALIPSO, 2011, Koffi et al., 2012). In contrast with the relatively stable lower troposphere in the winter season, boundary layer mixing, convection, and transport are enhanced in pre-monsoon season. As a result, aerosols are more efficiently mixed vertically, with Z_a in CALIOP increasing from 1.18 km in DJF to 2.18 km in MAM. The aerosol extinction near the surface in MAM is only half of its DJF values, and the fraction of AOD in the lowest 2 km is reduced from 87% in DJF to 60% in MAM when the aerosol vertical mixing is relatively uniform within the lowest 3 km and diminishes at higher altitude around 5-6 km. The profile during the monsoon season is similar to that in the pre-monsoon but with a lower value of Z_a as 2.02 km ; and the profile during the post-monsoon is similar to that in the winter but with a higher value of Z_a as 1.24 km .

Most models, especially GE5, capture the observed seasonal variation of Z_a (and $F_{2\text{km}}$) over Kanpur, with lower Z_a (higher $F_{2\text{km}}$) during the wintertime (DJF) and post-monsoon (ON), and higher Z_a (lower $F_{2\text{km}}$) during the pre-monsoon (MAM) and monsoon (JJAS) at all stations, although the profiles and magnitude are quite different

Xiaohua 1/13/2015 2:59 PM

Deleted: flow ...ignificantly become ... [1]

Xiaohua 1/13/2015 3:01 PM

Deleted: modeled vertical ...erosol ... [2]

Xiaohua 1/23/2015 3:05 PM

Deleted: CALIPSO...observed sea ... [3]

583 | from those of CALIOP. At Kanpur in DJF, most models (except for HAD and GIE)
 584 | largely underestimate AOD by 57% (ECH) to 85%(SPR), in particular the extinction
 585 | coefficient in the lowest 2 km, with F_{2km} varying from 68% (GIM) to 87% (GE5) among
 586 | these 5 models in contrast to 87% in CALIOP (Fig. 8a). At Hyderabad in central India
 587 | during the winter (DJF) and the post-monsoon (ON), models agree better with the
 588 | CALIOP. Different from CALIOP and other models, HAD produces extremely high
 589 | extinction coefficients close to the surface at Kanpur throughout all seasons, a factor of
 590 | 2 greater than CALIOP in DJF and a factor of 10 greater in ON. The models GIE and
 591 | GIM are a factor of 4 and 7 greater than CALIOP in JJAS, respectively. In addition, GIE
 592 | exhibits extremely large extinction coefficients between 2 and 3 km in all seasons,
 593 | which is not found in CALIOP. This discrepancy is associated with problems in the
 594 | simulation of nitrate in this model.

4.5 Monthly BC surface concentration

597 | Figure 9 shows observed and modeled monthly surface BC concentration in 2006 (2005
 598 | from model ECH) at 8 ICARB stations. In general, the magnitude of BC surface
 599 | concentrations is closely related to the strength of emission source, with higher values
 600 | in northern India, gradually decreasing southward. In particular, the highest BC surface
 601 | concentration is found in the largest Indian city Delhi, with a value of $27\mu\text{g m}^{-3}$ in
 602 | January. In contrast, BC surface concentration is lower in the remote sites, such as the
 603 | island sites (Minicoy and Port Blair) and mountain site (Nainital), not exceeding $2.6\mu\text{g m}^{-3}$.
 604 | The surface BC concentration exhibits pronounced seasonal variation, with higher
 605 | values found in the winter and post-monsoon seasons and lower values in the spring
 606 | and summer. We attribute this temporal variability to the seasonal variations of emission
 607 | sources, ABL (affecting vertical mixing), and rainfall (removing BC from the atmosphere).
 608 | It was reported by previous studies that total BC loading over South Asia mainly comes
 609 | from biofuel emissions in winter along with coal burning in the vicinity of the
 610 | measurement location (e.g. Ali et al., 2004; Singh et al., 2008; Beegum et al., 2009;
 611 | Srivastava et al., 2012b). Overall, modeled BC surface concentrations at all stations
 612 | except Nainital (a mountain site) are too low especially in winter, varying from near zero
 613 | to $6\mu\text{g m}^{-3}$. In particular, in Delhi and Hyderabad - two very large cities (see Table 2), all
 614 | models show a pronounced low bias in the winter, capturing only 3%-19% of the
 615 | observed values. The simulated BC surface concentrations are found to have a better
 616 | agreement at Kharagpur, where models capture 20%-100% of the observed value. This
 617 | contrast is possibly due to the fact that BC loading at Kharagpur mainly comes from
 618 | coal-fired power plants (Nair et al., 2007), which are relatively well represented in the
 619 | emission data (discussed in Section 5.3). At Minicoy and Port Blair, where the observed
 620 | BC concentration are relatively lower, models agree better with ICARB, capturing about
 621 | 10%-38% of the observed values. The underestimation of BC found in the urban city
 622 | (e.g. Delhi) could partly attribute to the fact that a global model with a coarse spatial
 623 | resolution is difficult to reproduce pollutant concentrations measured in a point station

Xiaohua 1/13/2015 3:08 PM

Deleted: SO

Xiaohua 1/13/2015 3:09 PM

Deleted: 8

Xiaohua 1/13/2015 3:09 PM

Deleted: SO

Xiaohua 1/13/2015 3:09 PM

Deleted: SO relatively better

Xiaohua 1/13/2015 3:09 PM

Deleted: SO

Xiaohua 1/13/2015 3:30 PM

Deleted: about

Xiaohua 1/13/2015 3:27 PM

Deleted: of

Xiaohua 1/13/2015 3:10 PM

Deleted: S

Xiaohua 1/13/2015 3:10 PM

Deleted: O

Xiaohua 1/13/2015 3:29 PM

Deleted: , so do

Xiaohua 1/13/2015 3:30 PM

Deleted: in JJAS

Xiaohua 1/13/2015 3:29 PM

Deleted: about

Xiaohua 1/13/2015 3:29 PM

Deleted: of

Xiaohua 1/13/2015 3:10 PM

Deleted: SO

Xiaohua 1/13/2015 3:31 PM

Deleted: there is an abnormal increase of extinction coefficient between 2km-3km in model GIE in all seasons and stations, associated with problems in the nitrate simulation in this model.

Xiaohua 1/23/2015 3:11 PM

Deleted: In addition, t

Xiaohua 1/23/2015 1:33 PM

Deleted: boundary layer depth

Xiaohua 1/23/2015 3:12 PM

Deleted: in winter

Xiaohua 1/14/2015 1:31 PM

Deleted: 2

Xiaohua 1/23/2015 11:51 AM

Deleted: It should be noted that it is difficult for

under urban environment. However, the underestimations of BC surface concentration are found in those background stations as well (e.g. over the mountain site of Nainital and the island sites of Minicoy and Port Blair). In addition, modeled AODs are found too low in comparison not only with AERONET point observations, but also with the level-3 multiple satellite data from MODIS, SeaWiFS (both 1°x1° resolution) and MISR (0.5°x0.5° resolution) on regional scales, as shown earlier in Fig. 5 and Fig. 7. Therefore, the underestimations of modeled BC and AOD together in the wintertime are more likely due to other factors, as discussed later in Section 5, than scaling.

5. Possible causes of the aerosol underestimations

As shown above, AOD, AAOD and BC surface concentration are consistently underestimated during the wintertime and the post-monsoon season by the seven global models used in this study. Such underestimation seems to be a quite common problem in other models as well, as shown in other previous studies (e.g. Dickerson et al., 2002; Reddy et al., 2004; Chin et al., 2009; Ganguly et al., 2009; Goto et al., 2011; Cherian et al., 2013). In particular, AOD and BC surface concentrations are most severely underestimated over the IGP (the main region of anthropogenic emissions). Several possible causes for these underestimates are suggested as below.

5.1 Wintertime relative humidity (RH) over the IGP

Foggy days with high humidity are very common during the wintertime over the IGP region (Gautam et al., 2007). For example, Kanpur was subjected to heavy fog or haze for about >65% days in the month of December 2004 (Tripathi et al., 2006), with averaged surface RH averaged about 75% and the surface temperature about 14.6°C. Low precipitation thus low wet removal in winter further contributes to accumulation of aerosols (Tripathi et al., 2006).

Figure 10 shows the comparisons between seven models and in-situ measurements from the ISRO-GBP land campaign at four stations in the IGP for December 2004. Comparisons are shown for surface meteorological conditions (RH and temperature); surface aerosol concentrations of SO_4^{2-} , NO_3^- , OA and BC; and column AOD and AAOD. AOD in the models are only 10% to 50% of the observed values at Kanpur. Interestingly, we found that RHs in six of the seven models (all except for HAD) only range from 11 to 35%, much lower compared to the measured RH of 75%. This large underestimation of RH could be partly due to the warm biases of air temperature about 1.7-7.5 °C across models (thus high bias of saturation water vapor pressure and low bias of RH). Under such dry conditions, the hygroscopic growth of soluble aerosols is suppressed. For example, if RH increases from the model averaged 21% to the observed 75%, mass extinction efficiencies (MEE) of SO_4^{2-} would be doubled, and those of OC and NO_3^- would be enhanced by 50% (Fig. 11). Note that NO_3^- is to be added to GE5.

Xiaohua 1/23/2015 11:58 AM

Deleted: n

Xiaohua 1/23/2015 12:00 PM

Deleted: ,

Xiaohua 1/23/2015 11:53 AM

Deleted: though it is more reasonable to expect these kinds of models to capture

Xiaohua 1/13/2015 3:35 PM

Comment [1]: Please refer to the response to reviewer 2.

Xiaohua 1/23/2015 3:36 PM

Moved down [2]: Interestingly, despite the low bias of BC concentration, most models reproduce the seasonal variation patterns at these sites with higher concentrations in winter and lower concentrations in summer, similar to what was pointed out in a recent study that compared the ICARB BC data with two models (Moorthy et al., 2013).

Xiaohua 1/23/2015 3:16 PM

Deleted: the

Xiaohua 1/13/2015 4:20 PM

Deleted:

Xiaohua 1/13/2015 4:23 PM

Deleted: Compared with the measured RH of 75% at Kanpur,

Xiaohua 1/13/2015 4:23 PM

Deleted: the

Xiaohua 1/23/2015 3:18 PM

Deleted: is

Xiaohua 1/13/2015 3:36 PM

Deleted: found significantly low, only 11-35 %

Xiaohua 1/13/2015 3:39 PM

Comment [2]: To account for this, why not compare absolute humidity? If that comparison is good, then it's a T problem. Response: the observational absolute humidity is not available.

Xiaohua 1/23/2015 3:21 PM

Deleted: in models GE5 and GOC,

Xiaohua 1/23/2015 3:21 PM

Deleted: almost

Xiaohua 1/13/2015 3:37 PM

Deleted: half,

Xiaohua 1/23/2015 3:20 PM

Deleted: if RH increases from the model averaged 21% to the observed 75%

In addition, foggy conditions favor the formation of secondary inorganic aerosol through enhanced aqueous-phase reaction in fog or cloud, which were supported by the observation that increased aerosol number concentration and surface concentrations of SO_4^{2-} and NO_3^- were found at Delhi (Tare et al., 2006), Hisar, and Allahabad (Ram et al., 2012), all in the IGP, under foggy conditions compared to hazy conditions. High RH and lower temperature in the winter also favor the formation of NH_4NO_3 by the reaction of nitric acid (HNO_3) and NH_3 (Lewandowska et al., 2004). Therefore, the lack of foggy conditions in current models would suppress such aqueous phase reactions in the winter. It is not surprising that the surface mass concentrations of SO_4^{2-} and NO_3^- in models are found much lower than the observed values as shown in Fig. 10. All models underestimate the surface concentration of SO_4^{2-} , capturing merely from 5% (GIE and GIM) to 50% (GE5) of the observed value. Among three models that include NO_3^- , GIE and GIM produce extremely low NO_3^- concentrations that are only 0.1% of the observed amount, and HAD captures about 38% of the observed NO_3^- . Of course, these underestimations of surface aerosol concentrations might be caused by other reasons as well, such as possible low-biases of anthropogenic emission amounts in models as discussed in following Section 5.3, however, the lack of foggy conditions in models is a critical defect.

5.2 Nitrate component

At all 4 stations, the surface concentrations of NO_3^- are comparable to those of SO_4^{2-} (e.g. $14.9 \mu\text{g m}^{-3}$ of SO_4^{2-} and $15.7 \mu\text{g m}^{-3}$ of NO_3^- at Kanpur). However, only three models include NO_3^- component. Among them, GIE and GIM produce extremely low NO_3^- concentrations that are only 0.1% of the observed amount at Kanpur. HAD captures about 38% of the observed NO_3^- . Interestingly, among all models, AOD simulated by HAD is the closest to the observations during the winter, which is not only apparent at 4 stations in IGP (Kanpur, Agra, Allahabad and Hisar) (Fig. 10) but also over entire South Asia (Fig. 7b). This agreement is associated with its inclusion of NO_3^- (Fig. 6) and aforementioned high relative humidity in Section 5.1. This evidence reveals the significant contribution of NO_3^- to the high AOD observed over IGP region in the winter and suggests that NO_3^- component should be included at least in a model in order to adequately represent the total AOD over South Asia.

5.3 Anthropogenic/Biofuel emission amounts and seasonal variation

At Kanpur, the models also largely underestimate surface OA and BC concentration, capturing only from 8% (GIE and GIM) to 60%(GE5) of the observed OA values, and 8% (GIE and GIM) to 46% (SPR) of the observed BC values, respectively. The surface concentrations of all species are rather low in the two GISS models (GIE and GIM), usually less than 10% of observed values. As shown in Fig. 10, the underestimations of surface concentrations by these models are similar at other stations in the IGP, i.e. Agra,

Xiaohua 1/23/2015 3:23 PM

Deleted: .

Xiaohua 1/23/2015 3:24 PM

Deleted: T

Xiaohua 1/13/2015 4:49 PM

Deleted: , and the exclusion of nitrate aerosols in some of the models would further contribute to the low bias of wintertime AOD

Xiaohua 1/13/2015 4:54 PM

Deleted: 2

Xiaohua 1/13/2015 5:07 PM

Deleted: At Kanpur, the observed surface concentration of SO_4^{2-} is $14.9 \mu\text{g m}^{-3}$ and NO_3^- is $15.7 \mu\text{g m}^{-3}$ as shown in Fig. 10. All models underestimate the surface concentration of SO_4^{2-} , capturing merely 5% (GIE and GIM) to 50% (GE5) of the observed SO_4^{2-} . Among the three models that include NO_3^- , GIE and GIM produces extremely low NO_3^- concentrations that is only 0.1% of the observed amount, whereas HAD captures about 38% of the observed NO_3^- . Interestingly, among all models, AOD simulated by HAD is the closest to the observations during the winter, which is not only apparent at 4 stations in IGP (Kanpur, Agra, Allahabad and Hisar) (Fig. 10) but also over entire South Asia (Fig. 7a). This is closely associated with its inclusion of NO_3^- (Fig. 6) and aforementioned high relative humidity (Fig. 10). This evidence suggests the contribution of RH and NO_3^- to the high AOD observed over IGP region in the winter. Meanwhile, the model discrepancies also suggests that the simulations of NO_3^- and SO_4^{2-} need to be improved in all models, especially NO_3^- that should be included or improved. At

790 Allahabad and Hisar, which differ from Kanpur as being semi-urban and less populated.
 791 Therefore, the results above suggest that the anthropogenic emissions used by the
 792 models (i.e., A2-ACCMIP and A2-MAP) are likely biased low. For comparison, BC
 793 emissions **in year 2000** over India **from** A2-ACCMIP and A2-MAP are **0.5 Tg yr⁻¹**, at the
 794 low end of a group of emission inventories shown in Granier et al. (2011), with 40% or
 795 0.3 Tg yr⁻¹ lower than those considered by REAS and GAINS-2008 emission inventories
 796 (Fig. 5a in Granier et al., 2011). A study by Nair et al. (2012) reported that the simulated BC
 797 surface concentration at Kharagpur agreed better with the observations using REAS.

798 Different from other regions in northern hemisphere where fossil fuel burning and
 799 industrial processes tend to dominate, biofuel (about 27.0% energy usage in 2007) and
 800 open biomass burning in South Asia contribute two-thirds of carbon-containing aerosols
 801 to form the dense brown clouds in the winter (Gustafsson et al., 2009). Over India, 42%
 802 of total BC emission is from biofuel, which is believed to be the largest source of BC,
 803 with the **remaining** 33% from open biomass burning and 25% from fossil fuel
 804 (Venkataraman et al., 2005). This is because the incomplete combustion of residential
 805 heating and cooking (burning of wood, paper or other solid wastes) is quite common in
 806 South Asia, especially among the underprivileged, leading to large amount of smoke
 807 comprised mainly of black carbon and condensed semi-volatile organics. We have
 808 found in this study that the simulated BC surface concentrations agree better with the
 809 observations at Kharagpur than at Delhi (Fig. 9). As reported by Prasad et al. (2006),
 810 the sources of BC at Kharagpur located in eastern IGP were mainly linked to the
 811 clusters of the coal-based industries there, while mainly linked to combustion of biofuel
 812 at Delhi in western IGP. This contrast is most pronounced in the winter when residential
 813 heating is highly demanded, leading to enhanced emissions of biofuel. As another
 814 evidence, the ratios of OC/BC were reported as high as 8.0±2.2 at Allahabad (Ram et
 815 al., 2012) and 8.5±2.2 at Hisar (Rengarajan et al., 2007) during December 2004,
 816 indicating a major emission source from biomass combustions, such as from biofuel
 817 (Husain et al., 2007). However, in the models studied in this paper, the ratios range from
 818 only 0.44–4.02 at Allahabad and 0.58–3.80 at Hisar, indicating a domination of source
 819 from fossil fuel instead (Husain et al., 2007). In sum, the underestimation of
 820 anthropogenic emission in South Asia is more likely attributed to the underestimation of
 821 biofuel combustion.

822 In addition, the anthropogenic emissions of both A2-ACCMIP and A2-MAP
 823 emission datasets used by models in this study are constant throughout each year. The
 824 lack of seasonal variation would amplify the underestimation of aerosol amount found in
 825 models during the winter, when more biofuels are consumed for heating. In fact, the
 826 uncertain and inadequate representations of aerosol emissions over South Asia have
 827 been pointed out by other studies as well (e.g. Sahu et al., 2008; Ganguly et al., 2009;
 828 Nair et al., 2012; Lawrence and Lelieveld, 2010).

Xiaohua 1/13/2015 3:51 PM

Deleted: year 2000

Xiaohua 1/13/2015 3:51 PM

Deleted: in

Xiaohua 1/13/2015 3:51 PM

Deleted: about

Xiaohua 1/13/2015 5:09 PM

Deleted: rest

Xiaohua 1/13/2015 5:11 PM

Moved down [1]: In sum, the underestimation of anthropogenic emission in South Asia is likely attributed more to the biofuel combustion.

Xiaohua 1/13/2015 5:11 PM

Moved (insertion) [1]

5.4 Agriculture waste burning emissions

The extensive agriculture waste burning during post-monsoon season (October-November) after harvest in northwest India (e.g., Punjab) makes a large contribution to the enhanced dense haze over South Asia in this season. The agricultural fire in this area is evident in the MODIS fire count product, which is responsible for the high AOD shown in the satellite products (Vadrevu et al., 2011; Sharma et al., 2010). The smoke from Punjab also impacts the downwind regions by eastward transport along IGP and southward to central-south India (Sharma et al., 2010; Badarinath et al., 2009a, b).

The monthly BC emission from open biomass burning used by most models is 0.011Tg C yr^{-1} during the post-monsoon season over South Asia, only about 2% of that from anthropogenic emission (comparing Fig. 3 and Fig. 2). In particular around Lahore, an AERONET station over the northwestern “breadbasket” agriculture region, the open biomass burning emission of BC is only around $0.03\text{ gC m}^{-2}\text{ yr}^{-1}$, less than 10% of that from anthropogenic emission. Such small amount of open biomass burning emission is indeed questionable because the BC emissions from open biomass burning should be comparable to that from anthropogenic emissions in November, considering a significant enhanced AAOD observed at Lahore in this season (Fig. 5). The underestimation of BC emission from agriculture waste burning implies a similar degree of underestimation of OC from the same source. Therefore, it is not surprising that all models fail to capture high AAOD and AOD in this season (Fig. 5 and Fig. 7d).

The open biomass burning emission datasets used in all models during our study period (2000-2007) are based on Global Fire Emissions Database Version 2 (GFED2), which is derived from MODIS burned area products. However, it was previously reported that the small fires such as agricultural waste burning were largely missing in the current GFED product (e.g. van der Werf et al., 2010; Randerson et al., 2012). The area burned in agricultural waste burning area are usually underestimated because the size of agriculture fires is so small that may not generate detectable burned scars in the 500 meter pixel resolution of MODIS product (van der Werf et al., 2010; Randerson et al., 2012).

5.5 Other factors

Other factors also can cause the model underestimation of AOD. For example, the observed ratio of water-soluble organic carbon (WSOC) to OC varied from 0.21 to 0.65, suggesting a significant contribution from secondary organic aerosols (SOAs) in India (Ram and Sarin et al., 2010). Enhanced SOA production was actually observed during fog episodes (Kaul et al., 2011). However, only two out of seven models include a detailed SOA chemistry. In addition, although the dust emission is minimal compared with anthropogenic emissions during the wintertime, the mineral sources such as silicates and alumina could be from road traffic dust and soil re-suspension, construction activity in the urban regions of the IGP (Tiwari et al., 2009). However, current models do not include these anthropogenic dust emissions yet.

Xiaohua 1/13/2015 4:54 PM

Deleted: 3

Xiaohua 1/13/2015 4:54 PM

Deleted: 4

Xiaohua 1/23/2015 3:35 PM

Deleted: can

882 Some difficulties with the models might be associated with the coarse spatial
883 resolution (i.e. coarser than 1 degree). Considering the terrain over South Asia,
884 especially the valley-type topography of the IGP region with the towering Himalaya in
885 the north, the aerosol processes may not be adequately represented at such coarse
886 spatial resolution. In addition, because of the non-linearity of wind-dependent dust
887 emission and RH-dependent aerosol hygroscopic growth, a finer model spatial
888 resolution will result in a higher dust emission and AOD (Bian et. al 2009). The
889 observed urban pollution levels at stations, such as Kanpur and Delhi, are expected to
890 be lower in a model box with a coarse spatial resolution (e.g. 1 degree) than a fine one
891 (e.g. half degree).

892 Despite the low bias of BC concentration, most models reproduce the seasonal
893 variation patterns at these sites with higher concentrations in winter and lower
894 concentrations in summer, similar to what was pointed out in a recent study that
895 compared the ICARB BC data with two models (Moorthy et al., 2013). In their study, a
896 regional model captured better the magnitude of BC concentration than GOCART
897 model that is also used in our study, thus an improvement on ABL scheme in GOCART
898 was recommended. The ABL is an important factor to determine the surface concentration of
899 aerosols, besides the factor of strength of emission sources. In winter, the averaged ABL is 400-
900 500 meters in the model GOCART (similar meteorological data used by GEOS5), about twice of
901 the observed ABL (Tripathi et al., 2006; Nair et al. 2007), thus a better-constrained ABL in
902 GOCART and GEOS5 could be helpful as suggested in the study by Moorthy et al. (2013).
903 Unfortunately we don't have ABL information from other models, so it is hard to address this
904 point for other models. Here, we would like to add that the column AAOD during wintertime is
905 underestimated as well, although in a less degree than surface concentration (by a factor of 3
906 verse 10). Thus underestimations of both BC surface concentration and AAOD indicate a
907 fundamental problem—BC emissions in wintertime might be underestimated in these models as
908 addressed in Section 5.3.

909 Interestingly, the models with the same anthropogenic emissions and biomass
910 burning emissions produce quite different results. At Kanpur in December 2004, for
911 example, surface concentration of OA in the model SPR is 10 times as large as that in
912 GIM (Fig. 10), which uses the same anthropogenic emission data, A2-ACCMIP.
913 Additionally, surface concentration of BC in SPR is 6 times as large as that in GIM (Fig.
914 10). Two other models, HAD and GOC, use the same A2-MAP emissions, but have
915 noticeably different seasonal variations of sulfate AOD (Fig. 6). Although, the emission
916 amount usually determines the magnitude of aerosols concentration in the atmosphere,
917 it plays little role in explaining the large model diversity. Instead, the differences in the
918 treatment of atmospheric processes (e.g., wet removal, dry deposition, cloud convection,
919 aqueous-phase oxidation and transport), assumptions of particle size, mixture, water
920 uptake efficiency, and optical properties are more responsible for the inter-model
921 differences.

922

Xiaohua 1/13/2015 5:12 PM

Deleted: feature

Xiaohua 1/23/2015 3:36 PM

Moved (insertion) [2]

Xiaohua 1/23/2015 3:42 PM

Deleted: Interestingly, d

Xiaohua 1/23/2015 3:36 PM

Formatted: None, Indent: First line: 0"

Xiaohua 1/23/2015 4:14 PM

Formatted: Not Highlight

Xiaohua 1/23/2015 3:36 PM

Deleted:

Xiaohua 1/13/2015 5:13 PM

Deleted: Albeit

Xiaohua 1/13/2015 5:14 PM

Deleted: ies

6. Conclusions

In this study, the aerosol simulations for 2000-2007 from seven global models are evaluated with satellite data and ground-based measurements over South Asia, in particular over Northern India (i.e. IGP), one of the heavily polluted regions in the world. The high AOD over the IGP is associated with high aerosol and precursor gas emissions (such as dust, SO_2 , NO_x , NH_3 , OA and BC) from local and upwind regions, and its valley-type topography (bounded by the towering Himalaya), favorable for accumulation of both anthropogenic and dust aerosols in this region. The main results of this study are summarized as below.

1. Averaged over the entire South Asia for 2000-2007, the annual mean AOD is about 0.281-0.355 from satellites retrievals. Six out of seven models consistently underestimate the annual mean AOD by 18%-45% compared to MISR, the lowest bound of four satellite datasets. The model performances are worse over northern India where the AOD from the same six models underestimate the annual mean AOD by 20-56% compared to MISR.
2. In general, the underestimations are mainly found during the winter and post-monsoon months when anthropogenic and open biomass burning emissions are dominant. During wintertime (DJF), six out of seven models largely underestimate AOD over Indian subcontinent. For example, these six models underestimate AOD by a factor of 4 and AAOD by a factor of 2 relative to AERONET at Kanpur, and the largest underestimations of aerosols occur in the lowest 2 km based on the comparisons with aerosol extinction profiles from CALIOP. During the winter and post-monsoon season, BC surface concentrations are severely underestimated at urban cities (such as Delhi) with the models capturing only 3%-19% of the observed values. Performance is better at remotes island sites (such as Minicoy and Port Blair) with the models capturing about 10%-38% the observed values.
3. The surface mass concentrations of all species (SO_4^{2-} , NO_3^- , OA and BC) in the wintertime simulated by models are as small as 0.1-60% of the observed values, indicating that the mass loading of aerosol is likely underestimated in all these models. In addition to the fact that the AOD and AAOD are also underestimated, it is very likely that anthropogenic emission, especially from biofuel, during the winter is underestimated in the emission dataset (A2-ACCMIP or A2-MAP). The lack of seasonal variation of emissions amplifies the discrepancies in winter.
4. It was also found that the surface concentration of NO_3^- is comparable with SO_4^{2-} at Kanpur and even higher at Agra in observations. However, NO_3^- is either not considered or significantly underestimated by the models, suggesting a need to better represent NO_3^- in the models.
5. The wintertime near-surface relative humidity is found to be significantly low with the model averaged 20% compared to the observed 70% in six out of seven models in IGP, which is associated with warm biases found in air temperature. As a result, the

Xiaohua 1/13/2015 3:15 PM

Deleted: vertical

hygroscopic growth of soluble aerosols and formation of secondary inorganic aerosol (NO_3^- and SO_4^{2-}) can be underestimated, which may further lead to an underestimation of AOD in these models.

6. During the post-monsoon season (ON), none of the models capture the observed high AOD over western and central IGP. Such discrepancy is attributed largely to the underestimation of open biomass burning in the emission inventory, which misses the aerosol emissions from agricultural waste burning.

In summary, it remains a challenge for global models to **realistically** represent the aerosol distributions, loadings and seasonal cycles in South Asia, due to our limited knowledge of the aerosol sources and physical and optical properties, as well as unconstrained model parameters to adequately represent the atmospheric processes. This study identifies the major discrepancies associated with aerosol simulation in state-of-the-art global climate models, and suggests some directions to improve model simulation over South Asia by improving temperature and relative humidity in the meteorological fields, revising biofuel and agriculture fire emission dataset, and including/improving NO_3^- (and SOA). Moreover, more systematic measurements, especially long-term surface and vertical characterization of aerosol composition, precursor gases, optical properties, and meteorological fields (such as temperature, winds, relative humidity), are needed. Realizing the importance of understanding the source of the bias, we are currently working on quantifying the problems with ranks of importance via a series model sensitivity studies using our own model (GEOS5), including change the model spatial resolution, emission strength, additional species, meteorological variables, etc. These sensitivity simulations will allow us to rank the importance of the bias sources, which is not possible to do with the AeroCom models but will definitely provide insights to diagnose the model problems and directions of improvements for all models. We will report the findings in our future publications.

Acknowledgement

We thank the ICARB, ISRO-GBP, and AERONET networks for making their data available. Site PIs and data managers of those networks are gratefully acknowledged. We also thank the Goddard Earth Science Data and Information Services Center for providing gridded satellite products of SeaWiFS, MISR, and MODIS through their Giovanni website, and the AeroCom data management for providing access to the global model output used in this study. Dr. Brigitte Koffi is appreciated for providing L3 CALIOP data. X. Pan is supported by an appointment to the NASA Postdoctoral Program at the GSFC, administered by Oak Ridge Associated Universities through a contract with NASA. The work by MC, HB, DK, and PC are supported by the NASA MAP and ACPMAP Programs. SEB and KT have been supported by the NASA MAP program (NN-H-04-Z-YS-008-N and NN-H-08-Z-DA-001-N). L. Pozzoli was supported by PEGASOS (FP7-ENV-2010-265148). Resources supporting this work were provided by the NASA High-End Computing (HEC) Program through the NASA Center for

1011 Climate Simulation (NCCS) at Goddard Space Flight Center. ECHAM5-HAMMOZ
1012 simulations were supported by the Deutsches Klimarechenzentrum (DKRZ) and the
1013 Forschungszentrum Juelich. We are grateful to two reviewers for their constructive and
1014 helpful comments.
1015

1016 References

1018 Ali, K., Momin, G.A., Tiwari, S., Safai, P.D., Chate, D.M., Rao, P.S.P.: Fog and precipitation
1019 chemistry at Delhi, North India. *Atmos. Environ.*, 38, 4215–4222, 2004.

1021 Badarinath, K.V.S., Kharol, S.K. and Sharma, A. R.: Long-range transport of aerosols from
1022 agriculture crop residue burning in Indo-Gangetic Plains—A study using LIDAR, ground
1023 measurements and satellite data, *J. Atmos. Sol. Terr. Phys.*, 71, 112– 120,
1024 doi:10.1016/j.jastp.2008.09.035, 2009a.

1026 Badarinath, K.V.S., Kharol, S.K., Sharma, A.R., V. Krishna Prasad: Analysis of aerosol and
1027 carbon monoxide characteristics over Arabian Sea during crop residue burning period in the
1028 Indo-Gangetic Plains using multi-satellite remote sensing datasets, *J. Atmos. Solar-Terr.*
1029 *Phys.*, 71, 1267 – 1276, 2009b.

1031 Babu, S. S., Manoj, M. R., Moorthy, K. K., Gogoi, M. M., Nair, V. S., Kumar Kompalli, S.,
1032 Satheesh, S. K., Niranjana, K., Ramagopal, K., Bhuyan, P. K., and Singh, D.: Trends in
1033 aerosol optical depth over Indian region: potential causes and impact indicators, *J. Geophys.*
1034 *Res. Atmos.*, 118, 11794–11806, doi:10.1002/2013JD020507, 2013.

1036 v Bauer, S.E., Wright, D., Koch, D., Lewis, E.R., McGraw, R., Chang, L.-S. Schwartz, S.E.
1037 and Ruedy, R.: MATRIX (Multiconfiguration Aerosol TRacker of mIXing state): An aerosol
1038 microphysical module for global atmospheric models. *Atmos. Chem. Phys.*, 8, 6603-6035,
1039 doi:10.5194/acp-8-6003-2008, 2008.

1041 Bauer, S.E., Menon, S., Koch, D., Bond, T.C., and Tsigaridis, K.: A global modeling study
1042 on carbonaceous aerosol microphysical characteristics and radiative forcing. *Atmos. Chem.*
1043 *Phys.*, 10, 7439-7456, doi:10.5194/acp-10-7439-2010, 2010.

1045 Beegum, S., Moorthy, S.N., Babu, K.K., Satheesh, S.S., Vinoj, S.K., Badarinath, V., Safai,
1046 K.V.S., Devara, P.D., Singh, P.C.S., Vinod, S., Dumka U. C., Pant, P.: Spatial distribution
1047 of aerosol black carbon over India during pre-monsoon season. *Atmos. Environ.* 43,
1048 071e1078, 2009.

1050 Bellouin, N., Rae, J., Jones, A., Johnson, C., Haywood, J. and Boucher, O.: Aerosol forcing
1051 in the Climate Model Intercomparison Project (CMIP5) simulations by HadGEM2-ES and
1052 the role of ammonium nitrate, *J. Geophys. Res.*, 116, D20206, doi:10.1029/2011JD016074,
1053 2011.

1055 Bian, H., Chin, M., Rodriguez, J., Yu, H., Penner, J. E., Strahan, S.: Sensitivity of aerosol
1056 optical thickness and aerosol direct radiative effect to relative humidity, *Atmos. Chem. Phys.*,
1057 9, 2375-2386, 2009.

Xiaohua 1/14/2015 1:44 PM

Deleted: Babu, S. S. et al.: Trends in
aerosol optical depth over Indian region:
Potential causes and impact indicators, *J.*
Geophys. Res. Atmos., 118, 11,794–
11,806, doi:10.1002/2013JD020507, 2013.

1064 Cherian, R., Venkataraman, C., Quaas, J. and Ramachandran, S.: GCM simulations of
 1065 anthropogenic aerosol-induced changes in aerosol extinction, atmospheric heating and
 1066 precipitation over India, J. Geophys. Res. Atmos., 118, 2938–2955,
 1067 doi:10.1002/jgrd.50298, 2013.
 1068
 1069 Chin, M., Ginoux, P., Kinne, S., Torres, O., Holben, B. N., Duncan, B. N., Martin, R. V.,
 1070 Logan, J. A., Higurashi, A. and Nakajima, T.: Tropospheric aerosol optical thickness from
 1071 the GOCART model and comparisons with satellite and sun photometer measurements, J.
 1072 Atmos., Sci., 59, 461-483, 2002.
 1073
 1074 Chin, M., Diehl, T., Dubovik, O., Eck, T. F., Holben, B. N., Sinyuk, A. and Streets, D. G. :
 1075 Light absorption by pollution, dust and biomass burning aerosols: A global model study and
 1076 evaluation with AERONET data, Ann. Geophys., 27, 3439- 3464, 2009.
 1077
 1078 Chin, M., Diehl, T., Tan, Q., Prospero, J. M., Kahn, R. A., Remer, L. A., Yu, H., Sayer, A. M.,
 1079 Bian, H., Geogdzhayev, I. V., Holben, B. N., Howell, S. G., Huebert, B. J., Hsu, N. C.,
 1080 Kim, D., Kucsera, T. L., Levy, R. C., Mishchenko, M. I., Pan, X., Quinn, P. K.,
 1081 Schuster, G. L., Streets, D. G., Strode, S. A., Torres, O., and Zhao, X.-P.: Multi-decadal
 1082 aerosol variations from 1980 to 2009: a perspective from observations and a global model,
 1083 Atmos. Chem. Phys., 14, 3657-3690, doi:10.5194/acp-14-3657-2014, 2014.
 1084
 1085 [Colarco, P. R., da Silva, A., Chin, M., and Diehl, T.: Online simulations of global aerosol](#)
 1086 [distributions in the NASA GEOS-4 model and comparisons to satellite and ground-based](#)
 1087 [aerosol optical depth, J. Geophys. Res., 115, D14207, doi:10.1029/2009JD012820, 2010.](#)
 1088
 1089
 1090 [CALIPSO: CALIPSO Quality Statements Lidar Level 3 Aerosol Profile Monthly Products Version](#)
 1091 [Release: 1.00, 2011.](#)
 1092 Das, S. K., Jayaraman, A., and Misra, A.: Fog-induced variations in aerosol optical and
 1093 physical properties over the Indo-Gangetic Basin and impact to aerosol radiative forcing,
 1094 Ann. Geophys., 26, 1345-1354, doi:10.5194/angeo-26-1345-2008, 2008.
 1095
 1096 Dickerson, R. R., Andreae, M. O., Campos, T., Mayol-Bracero, O. L., Neusuess, C. and
 1097 Streets, D. G.: Analysis of black carbon and carbonmonoxide observed over the Indian
 1098 Ocean: Implications for emissions and photochemistry, J. Geophys. Res., 107(D19), 8017,
 1099 doi:10.1029/2001JD000501, 2002.
 1100
 1101 Diehl, T., Heil, A., Chin, M., Pan, X., Streets, D., Schultz, M., and Kinne, S.: Anthropogenic,
 1102 biomass burning, and volcanic emissions of black carbon, organic carbon, and SO₂ from
 1103 1980 to 2010 for hindcast model experiments, Atmos. Chem. Phys. Discuss., 12, 24895-
 1104 24954, 2012.
 1105
 1106 Ganguly, D., Jayaraman, A., Rajesh, T. A. and Gadhavi, H.: Wintertime aerosol properties
 1107 during foggy and nonfoggy days over urban center Delhi and their implications for
 1108 shortwave radiative forcing, J. Geophys. Res., 111, D15217, doi:10.1029/2005JD007029,
 1109 2006.
 1110
 1111 Ganguly, D., Ginoux, P., Ramaswamy, V., Winker, D. M., Holben, B. N. and Tripathi, S. N.:
 1112 Retrieving the composition and concentration of aerosols over the Indo-Gangetic basin

Xiaohua 1/14/2015 1:44 PM

Deleted: Colarco, P., da Silva, A., Chin, M., and Diehl, T.: Online simulations of global aerosol distributions in the NASA GEOS-4 model and comparisons to satellite and ground-based aerosol optical depth, J. Geophys. Res., 115, D14207, 2010. .

1120 using CALIOP and AERONET data, *Geophys. Res. Lett.*, 36, L13806,
 1121 doi:10.1029/2009GL038315, 2009.
 1122
 1123 Gautam, R., Hsu, N. C., Kafatos, M. and Tsay, S.-C.: Influences of winter haze on fog/low
 1124 cloud over the Indo-Gangetic Plains, *J. Geophys. Res.*, 112, D05207,
 1125 doi:10.1029/2005JD007036, 2007.
 1126
 1127 Gautam R., Hsu, N. C., Lau, W. K.-M. and Yasunari, T. J.: Satellite observations of desert
 1128 dust-induced Himalayan snow darkening, *Geophys. Res. Lett.*, 40, 988–993,
 1129 doi:10.1002/grl.50226, 2013.
 1130
 1131 Girolamo, D. L., Bond, T. C., Bramer, D., Diner, D. J., Fetters, F., Kahn, R. A. Martonchik,
 1132 J. V., Ramana, M. V., Ramanathan, V. and Rasch, P. J.: Analysis of Multi-angle Imaging
 1133 SpectroRadiometer (MISR) aerosol optical depths over greater India during winter 2001–
 1134 2004, *Geophys. Res. Lett.*, 31, L23115, doi:10.1029/2004GL021273, 2004.
 1135
 1136 Goto, D., Takemura, T., Nakajima, T. and Badarinath, K. V. S.: Global aerosol model-
 1137 derived black carbon concentration and single scattering albedo over Indian region and its
 1138 comparison with ground observations, *Atmos. Environ.*, 45(19), 3277–3285, 2011.
 1139
 1140 Granier, C., Bessagnet, B., Bond, T., D'Angiola, A., van der Gon, H. D., Frost, G. J., Heil, A.,
 1141 Kaiser, J. W., Kinne, S., Klimont, Z., Kloster, S., Lamarque, J.-F., Lioussé, C., Masui, T.,
 1142 Meleux, F., Mieville, A., Ohara, T., Raut, J. C., Riahi, K., Schultz, M. G., Smith, S. J.,
 1143 Thompson, A., van Aardenne, J., van der Werf, G. R., and van Vuuren, D. P.: Evolution of
 1144 anthropogenic and biomass burning emissions of air pollutants at global and regional scales
 1145 during the 1980–2010 period, *Climatic Change*, 109, 163–190, doi:10.1007/s10584-011-
 1146 0154-1, 2011.
 1147
 1148 [Gustafsson, O., Krusa, M., Zencak, Z., Sheesley, R. J., Granat, L., Engstrom, E., Praveen,](#)
 1149 [P. S., Rao, P. S. P., Leck, C., and Rodhe, H.: Brown Clouds over South Asia: Biomass or](#)
 1150 [Fossil Fuel Combustion?, *Science*, 323, 495–498, 2009.](#)
 1151
 1152 Kaul D., Gupta T., Tripathi, S. N., Tare V. and Collett, J.: Secondary Organic Aerosol: A
 1153 Comparison between Foggy and Non-foggy Days, *Environmental Science and Technology*,
 1154 45 (17), 7307–7313, 2011.
 1155
 1156 Koffi, B., Schulz, M., Bréon, F.-M., Griesfeller, J., Winker, D., Balkanski, Y., Bauer, S.,
 1157 Berntsen, T., Chin, M., Collins, W. D., Dentener, F., Diehl, T., Easter, R., Ghan, S., Ginoux,
 1158 P., Gong, S., Horowitz, L. W., Iversen, T., Kirkevåg, A., Koch, D., Krol, M., Myhre, G., Stier,
 1159 P., and Takemura, T.: Application of the CALIOP layer product to evaluate the vertical
 1160 distribution of aerosols estimated by global models: AeroCom phase I results, *J. Geophys.*
 1161 *Res.*, 117, D10201, doi:10.1029/2011JD016858, 2012.
 1162
 1163 Holben, B.N., Eck, T.F., Slutsker, I., Tanre, D., Buis, J.P., Setzer, A., Vermote, E., Reagan,
 1164 J.A., Kaufman, Y.J., Nakajima, T., Lavenu, F., Jankowiak, I., Smirnov, A.: AERONET — a
 1165 federated instrument network and data archive for aerosol characterization. *Remote Sens.*
 1166 *Environ.* 66, 1–16, 1998.
 1167
 1168 Hsu, N. C., Tsay, S.-C., King, M. D., and Herman, J. R.: Deep Blue retrievals of Asian
 1169 aerosol properties during ACE-Asia, *IEEE T. Geosci. Remote Sens.*, 44, 3180–3195, 2006.

Xiaohua 1/14/2015 1:44 PM

Deleted: Gustafsson Ö., Krusa, M., Zencak, Z., Sheesley, R.J., Granat, L., Engström, E. et. al: Brown clouds over South Asia: Biomass or fossil fuel combustion? *Science*, 323, 495–498, 2009.

1175
1176 [Hsu, N. C., Gautam, R., Sayer, A. M., Bettenhausen, C., Li, C., Jeong, M. J., Tsay, S.-C.,](#)
1177 [and Holben, B. N.: Global and regional trends of aerosol optical depth over land and ocean](#)
1178 [using SeaWiFS measurements from 1997 to 2010, Atmos. Chem. Phys., 12, 8037–8053,](#)
1179 [doi:10.5194/acp-12-8037-2012, 2012.](#)
1180
1181 Husain, L., Dutkiewicz, V. A., Khan, A. J., Chin, M., and Ghauri, B. M.: Characterization of
1182 carbonaceous aerosols in urban air, Atmos. Environ., 41, 6872–6883, 2007.
1183
1184 Jethva, H., Satheesh, S. K., Srinivasan, J., and Krishnamoorthy, K.: How Good is the
1185 Assumption about Visible Surface Reflectance in MODIS Aerosol Retrieval over Land? A
1186 Comparison with Aircraft Measurements over an Urban Site in India, IEEE Transactions on
1187 Geoscience and Remote Sensing, 47(7), 2009.
1188
1189 Kahn, R. A., W.-H. Li, C. Moroney, D. J. Diner, J. V. Martonchik, and E. Fishbein: Aerosol
1190 source plume physical characteristics from space-based multiangle imaging, J. Geophys.
1191 Res., 112, D11205, doi:10.1029/2006JD007647, 2007.
1192
1193 [Kahn, R. A., Gaitley, B. J., Garay, M. J., Diner, D. J., Eck, T., Smirnov, A., and Holben, B.](#)
1194 [N.: Multiangle Imaging SpectroRadiometer global aerosol product assessment by](#)
1195 [comparison with the Aerosol Robotic Network, J. Geophys. Res., 115, D23209,](#)
1196 [doi:10.1029/2010JD014601, 2010.](#)
1197
1198 [Kaskaoutis, D. G., Singh, R. P., Gautam, R., Sharma, M., Kosmopoulos, P. G., Tripathi, S.](#)
1199 [N.: Variability and Trends of Aerosol Properties over Kanpur, Northern India Using](#)
1200 [AERONET Data \(2001–10\). Environ. Res. Lett. 7: 024003, doi: 10.1088/1748-](#)
1201 [9326/7/2/024003, 2012.](#)
1202
1203 Kaul, D.S., Gupta, T., Tripathi, S.N., Tare, V., Collett, J.L.: Secondary organic aerosol: a
1204 comparison between foggy and nonfoggy days, Environ Sci Technol. 45(17), 7307–13. doi:
1205 10.1021/es201081d, 2011.
1206
1207 Lau, K. M., Kim, M. K. and Kim, K. M.: Asian summer monsoon anomalies induced by
1208 aerosol direct forcing: The role of the Tibetan Plateau, Clim. Dyn., 26, 855–864, 2006.
1209
1210 Lau, K. M., Kim, M. K., Kim, K. M. and Lee, W. S.: Enhanced surface warming and
1211 accelerated snow melt in the Himalayas and Tibetan Plateau induced by absorbing
1212 aerosols, Env. Res. Lett., 5, 025204, doi:10.1088/1748-9326/5/2/025204, 2010.
1213
1214 Lawrence, M. G., and Lelieveld, J.: Atmospheric pollutant outflow from southern Asia: A
1215 review, Atmos. Chem. Phys., 10, 11,017–11,096, 2010.
1216
1217 Lewandowska, A., F. Lucyna, and B. Magdalena: Ammonia and ammonium over the
1218 southern Baltic Sea, part 2. The origin of ammonia and ammonium over two stations:
1219 Gdynia and Hel, Oceanologia, 46(2), 185– 200, 2004.
1220
1221 [Levy, R. C., Remer, L. A., Mattoo, S., Vermote, E. F., and Kaufman, Y. J.: Second-](#)
1222 [generation operational algorithm: Retrieval of aerosol properties over land from inversion of](#)

Xiaohua 1/14/2015 1:45 PM

Deleted: Hsu, N. C., Gautam, R., Sayer, A. M., Bettenhausen, C., Li, C., Jeong, M. J., Tsay, S.-C., and Holben, B. N.: Global and regional trends of aerosol optical depth over land and ocean using SeaWiFS measurements from 1997 to 2010, Atmos. Chem. Phys. Discuss., 12, 8465–8501, doi:10.5194/acpd-12-8465-2012, 2012.

Xiaohua 1/14/2015 1:45 PM

Deleted: Kaskaoutis D.G., Singh, R.P., Gautam, R., Sharma, M., Kosmopoulos, P.G., Tripathi, S.N.: Variability and trends of aerosol properties over Kanpur, northern India using AERONET data (2001–10) Environ. Res. Lett., 109, 2012.

1238 [Moderate Resolution Imaging Spectroradiometer spectral reflectance, J. Geophys.](#)
1239 [Res., 112, D13211, doi:10.1029/2006JD007811, 2007.](#)
1240
1241 Levy, R. C., Remer, L. A., Kleidman, R. G., Mattoo, S., Ichoku, C., Kahn, R., and Eck, T. F.:
1242 Global evaluation of the Collection 5 MODIS dark-target aerosol products over land, Atmos.
1243 Chem. Phys., 10, 10399–10420, doi:10.5194/acp-10-10399-2010, 2010.
1244
1245 Martonchik, J. V., Diner, D. J., Kahn, R., Gaitley, B. and Holben, B. N.: Comparison of MISR
1246 and AERONET aerosol optical depths over desert sites, Geophys. Res. Lett., 31, L16102,
1247 doi:10.1029/2004GL019807, 2004.
1248
1249 Menon, S., Koch, D., Beig, G., Sahu, S., Fasullo, J., and Orlikowski, D.: Black carbon
1250 aerosols and the third polar ice cap, Atmos. Chem. Phys., 10, 4559–4571, doi:10.5194/acp-
1251 10-4559-2010, 2010.
1252
1253 Moorthy, K. K., Beegum, S. N., Srivastava, N., Satheesh, S. K., Chin, M., Blond, N., Babu,
1254 S. S. and Singh, S.: Performance Evaluation of Chemistry Transport Models over India,
1255 Atmos. Environ., 71, 210–225, 2013.
1256
1257 Myhre, G., Samset, B. H., Schulz, M., Balkanski, Y., Bauer, S., Bernsten, T. K., Bian, H.,
1258 Bellouin, N., Chin, M., Diehl, T., Easter, R. C., Feichter, J., Ghan, S. J., Hauglustaine, D.,
1259 Iversen, T., Kinne, S., Kirkevåg, A., Lamarque, J.-F., Lin, G., Liu, X., Lund, M. T., Luo, G.,
1260 Ma, X., van Noije, T., Penner, J. E., Rasch, P. J., Ruiz, A., Seland, Ø., Skeie, R. B., Stier, P.,
1261 Takemura, T., Tsigaridis, K., Wang, P., Wang, Z., Xu, L., Yu, H., Yu, F., Yoon, J.-H., Zhang,
1262 K., Zhang, H., and Zhou, C.: Radiative forcing of the direct aerosol effect from AeroCom
1263 Phase II simulations, Atmos. Chem. Phys., 13, 1853–1877, doi:10.5194/acp-13-1853-2013,
1264 2013.
1265
1266 Nair, V. S., Moorthy, K. K., Alappattu, D. P., Kunhikrishnan, P. K., George, S., Nair, P. R.,
1267 Babu, S. S., Abish, B., Satheesh, S. K., Tripathi, S. N., Niranjana, K., Madhavan, B. L.,
1268 Srikant, V., Dutt, C. B. S., Badarinath, K. V. S., and Reddy, R. R.: Wintertime aerosol
1269 characteristics over the Indo-Gangetic Plain (IGP): Impacts of local boundary layer
1270 processes and long-range transport, J. Geophys. Res., 112, D13205,
1271 doi:10.1029/2006JD008099, 2007.
1272
1273 [Nair, V. S., Solmon, F., Giorgi, F., Mariotti, L., Babu, S. S., and Moorthy, K. K.: Simulation of](#)
1274 [South Asian aerosols for regional climate studies, J. Geophys. Res., 117, D04209,](#)
1275 [doi:10.1029/2011JD016711, 2012.](#)
1276
1277 Ohara, T., Akimoto, H., Kurokawa, J., Horii, N., Yamaji, K., Yan, X. and Hayasaka, T. : An
1278 Asian emission inventory of anthropogenic emission sources for the period 1980–2020,
1279 Atmos. Chem. Phys., 7, 4419–4444, 2007.
1280
1281 Pozzoli, L., Janssens-Maenhout, G., Diehl, T., Bey, I., Schultz, M. G., Feichter, J., Vignati,
1282 E., and Dentener, F.: Reanalysis of tropospheric sulphate aerosol and ozone for the period
1283 1980–2005 using the aerosol-chemistry-climate model ECHAM5-HAMMOZ, Atmos. Chem.
1284 Phys. Discuss., 11, 10191–10263, doi:10.5194/acpd-11-10191-2011, 2011.
1285

Xiaohua 1/14/2015 1:46 PM

Deleted: Nair, V. S., Solmon, F. , Giorgi, F., Mariotti, L., Babu, S. S. and Moorthy, K. K. : Simulation of South Asian aerosols for regional climate studies, J. Geophys. Res., 117, D04209, 2012. .

1291 Prasad, A. K., Singh, R. P., and Kafatos, M.: Influence of coal based thermal power plants
 1292 on aerosol optical properties in the Indo-Gangetic basin, *Geophys. Res. Lett.*, 33, L05805,
 1293 doi:10.1029/2005GL023801, 2006.
 1294
 1295 Qian, Y., Flanner, M. G., Leung, L. R. , and Wang W.: Sensitivity studies on the impacts of
 1296 Tibetan Plateau snowpack pollution on the Asian hydrological cycle and monsoon climate,
 1297 *Atmos. Chem. Phys.*, 11, 1929–48, doi:10.5194/acp-11-1929-2011, 2011.
 1298
 1299 Ram K., Sarin, M. M.: Spatio-temporal variability in atmospheric abundances of EC, OC and
 1300 WSOC over Northern India, *Journal of Aerosol Science*, 41(1), 88-98, 2010.
 1301
 1302 Ram, K., Sarin, M. M., Sudheer, A. K. and Rengarajan, R.: Carbonaceous and secondary
 1303 inorganic aerosols during wintertime fog and haze over urban sites in the Indo-Gangetic
 1304 Plain, *Aerosol Air Qual. Res.*, 12, 359–370, 2012.
 1305
 1306 Ramachandran, S., Rengarajan, R., Jayaraman, A., Sarin, M. M. and Das, S. K.: Aerosol
 1307 radiative forcing during clear, hazy, and foggy conditions over a continental polluted location
 1308 in north India, *J. Geophys. Res.*, 111, D20214, doi:10.1029/2006JD007142, 2006.
 1309
 1310 Ramachandran, S., and Cherian R.: Regional and seasonal variations in aerosol optical
 1311 characteristics and their frequency distributions over India during 2001–2005, *J. Geophys.*
 1312 *Res.*, 113, D08207, doi:10.1029/2007JD008560, 2008.
 1313
 1314 Ramachandran, S., and Kedia S.: Aerosol, clouds and rainfall: inter-annual and regional
 1315 variations over India, *Clim. Dyn.*, 40(7–8), 1591–1610, doi:10.1007/s00382-012-1594-7,
 1316 2013.
 1317
 1318 Ramanathan, V., Crutzen, P. J., Lelieveld, J., Mitra, A. P., Althausen, D., Anderson, J.,
 1319 Andreae, M. O., Cantrell, W., Cass, G. R., Chung, C. E., Clarke, A. D., Coakley, J. A.,
 1320 Collins, W. D., Conant, W. C., Dulac, F., Heintzenberg, J., Heymsfield, A. J., Holben, B.,
 1321 Howell, S., Hudson, J., Jayaraman, A., Kiehl, J. T., Krishnamurti, T. N., Lubin, D.,
 1322 McFarquhar, G., Novakov, T., Ogren, J. A., Podgorny, I. A., Prather, K., Priestley, K.,
 1323 Prospero, J. M., Quinn, P. K., Rajeev, K., Rasch, P., Rupert, S., Sadourny, R., Satheesh, S.
 1324 K., Shaw, G. E., Sheridan, P., and Valero, F. P. J.: Indian Ocean Experiment: An integrated
 1325 analysis of the climate forcing and effects of the great Indo-Asian haze, *J. Geophys. Res.*,
 1326 106, 28371–28398, 2001.
 1327
 1328 Ramanathan V., Chung C., Kim D., Bettge T., Buja L., Kiehl J.T., Washington W.M., Fu Q.,
 1329 Sikka D.R., Wild M.: Atmospheric brown clouds: impact on South Asian climate and
 1330 hydrologic cycle. *Proc Natl Acad Sci* 102:5326–5333, DOI 10.1073/pnas.0500656102, 2005.
 1331
 1332 Randerson, J. T., Chen, Y., van der Werf, G. R., Rogers, B. M., and Morton, D. C.: Global
 1333 burned area and biomass burning emissions from small fires, *J. Geophys. Res.*, 117,
 1334 G04012, doi:10.1029/2012JG002128, 2012.
 1335
 1336 Reddy, M. S., Boucher, O., Venkataraman, C., Verma, S., Le'on, J.-F., Bellouin, N., and
 1337 Pham, M.: General circulation model estimates of aerosol transport and radiative forcing
 1338 during the Indian Ocean Experiment, *J. Geophys. Res.*, 109, D16205,
 1339 doi:10.1029/2004JD004557, 2004.
 1340

1341 Rengarajan, R., Sarin, M. M., and Sudheer, A. K.: Carbonaceous and inorganic species in
 1342 atmospheric aerosols during wintertime over urban and high-altitude sites in North India, *J.*
 1343 *Geophys. Res.*, 112, D21307, doi:10.1029/2006JD008150, 2007.
 1344
 1345 Safai, P. D., Kewat, S., Pandithurai, G., Praveen, P. S., Ali, K., Tiwari, S., Rao, P. S. P.,
 1346 Budhawant, K. B., Saha, S. K., Devara, P. C. S.: Aerosol characteristics during winter fog at
 1347 Agra, North India. *J. Atmos. Chem.*, 61(2), 101–118, 2008.
 1348
 1349 Sahu, S. K., Beig, G., and Sharma, C.: Decadal growth of black carbon emissions in India,
 1350 *Geophys. Res. Lett.*, 35, L02807, doi:10.1029/2007GL032333, 2008.
 1351
 1352 Sanap, S.D., Ayantika, D.C., Pandithurai, G., Niranjana, K.: Assessment of the aerosol
 1353 distribution over Indian subcontinent in CMIP5 models, *Atmospheric Environment*, 87, 123–
 1354 137, 2014.
 1355
 1356 Sayer, A. M., Hsu, N. C., Bettenhausen, C., Ahmad, Z., Holben, B. N., Smirnov, A., Thomas,
 1357 G. E., and Zhang, J.: SeaWiFS Ocean Aerosol Retrieval (SOAR): algorithm, validation, and
 1358 comparison with other datasets, *J. Geophys. Res.*, 117, D03206, doi:10.1029/2011JD016599,
 1359 2012.
 1360
 1361 [Sayer, A. M., Hsu, N. C., Bettenhausen, C., and Jeong, M.-J.: Validation and uncertainty](#)
 1362 [estimates for MODIS Collection 6 “Deep Blue” aerosol data, *J. Geophys. Res.*](#)
 1363 [Atmos., 118, 7864–7872, doi:10.1002/jgrd.50600, 2013.](#)
 1364
 1365 [Sessions, W. R., Reid, J. S., Benedetti, A., Colarco, P. R., da Silva, A., Lu, S., Sekiyama, T.,](#)
 1366 [Tanaka, T. Y., Baldasano, J. M., Basart, S., Brooks, M. E., Eck, T. F., Iredell, M., Hansen, J.](#)
 1367 [A., Jorba, O. C., Juang, H.-M. H., Lynch, P., Morcrette, J.-J., Moorthi, S., Mulcahy, J.,](#)
 1368 [Pradhan, Y., Razingzer, M., Sampson, C. B., Wang, J., and Westphal, D. L.: Development](#)
 1369 [towards a global operational aerosol consensus: basic climatological characteristics of the](#)
 1370 [International Cooperative for Aerosol Prediction Multi-Model Ensemble \(ICAP-MME\), *Atmos.*](#)
 1371 [Chem. Phys.](#), 15, 335–362, doi:10.5194/acp-15-335-2015, 2015.
 1372
 1373 Sharma, A.R., Kharol, S.K., Badarinath, K.V.S., Singh, D.: Impact of agriculture crop
 1374 residue burning on atmospheric aerosol loading — a study over Punjab State, India. *Ann.*
 1375 *Geophys.* 28, 367–379, 2010.
 1376
 1377 Singh T., Khillare P.S., Shridhar V., Agarwal T.: Visibility impairing aerosols in the urban
 1378 atmosphere of Delhi. *Environ Monit Assess* 141:67–77, 2008.
 1379
 1380 Srivastava, A. K., Tripathi, S. N., Dey, S., Kanawade, V. P., and Tiwari, S.: Inferring aerosol
 1381 types over the Indo-Gangetic Basin from ground based sunphotometer measurements,
 1382 *Atmos. Res.*, 109–110, 64–75, doi:10.1016/j.atmosres.2012.02.010, 2012a.
 1383
 1384 Srivastava, A.K., Singh, S., Pant, P., Dumka, U.C.: Characteristics of black carbon over
 1385 Delhi and Manora Peak-a comparative study. *Atmos Sci Lett* 13:223–230.
 1386 doi:10.1002/asl.386, 2012b.
 1387
 1388 Takemura, T., Nozawa, T., Emori, S., Nakajima, T. Y., and Nakajima, T.: Simulation of
 1389 climate response to aerosol direct and indirect effects with aerosol transport-radiation model,
 1390 *J. Geophys. Res.-Atmos.*, 110, D02202, doi:10.1029/2004jd005029, 2005.

1391
 1392 Takemura, T., Egashira, M., Matsuzawa, K., Ichijo, H., O'Ishi, R., and Abe-Ouchi, A.: A
 1393 simulation of the global distribution and radiative forcing of soil dust aerosols at the Last
 1394 Glacial Maximum, *Atmos. Chem. Phys.*, 9, 3061–3073, doi:10.5194/acp-9-3061-2009, 2009.
 1395
 1396 [Tare, V., Tripathi, S.N., Chinnam, N., Srivastava, A.K., Dey, S., Manar, M., Kanawade, V.P.,](#)
 1397 [Agarwal, A., Kishore, S., Lal, R.B., Sharma, M.: Measurements of atmospheric parameters](#)
 1398 [during Indian Space Research Organization Geosphere Biosphere Program Land](#)
 1399 [Campaign II at a typical location in the Ganga Basin: 2. Chemical properties, *J. Geophys.*](#)
 1400 [Res., 111, D23210, doi:10.1029/2006JD007279, 2006.](#)
 1401
 1402 Tiwari, S., Srivastava, A.K., Bisht, D.S., Bano, T., Singh, S., Behura, S.,
 1403 Srivastava, M.K., Chate, D.M., Padmanabhamurty, B.: Black carbon and chemical
 1404 characteristics of PM₁₀ and PM_{2.5} at an urban site of North India. *J. Atmos. Chem.* 62(3),
 1405 193–209. doi:10.1007/s10874-010-9148-z, 2009.
 1406
 1407 Tripathi, S. N., Dey, S., Tare, V. and Satheesh, S. K.: Aerosol black carbon radiative forcing
 1408 at an industrial city in northern India, *Geophys. Res. Lett.*, 32, L08802,
 1409 doi:10.1029/2005GL022515, 2005.
 1410
 1411 Tripathi, S. N., Tare, V., Chinnam, N., Srivastava, A. K., Dey, S., Agarwal, A., Kishore, S.,
 1412 Lal, R. B., Manar, M., Kanwade, V. P., Chauhan, S. S. S., Sharma, M., Reddy, R. R., Gopal,
 1413 K. R., Narasimhulu, K., Reddy, L. S. S., Gupta, S., and Lal, S.:
 1414 Measurements of atmospheric parameters during Indian Space Research Organization
 1415 Geosphere Biosphere Programme Land Campaign II at a typical location in the Ganga
 1416 basin: 1. Physical and optical properties, *J. Geophys. Res.*, 111, D23209,
 1417 doi:10.1029/2006JD007278, 2006.
 1418
 1419 Tsigaridis, K., Koch, D. M., and Menon, S.: Uncertainties and importance of sea-spray
 1420 composition on aerosol direct and indirect effects, *J. Geophys. Res.*, 118, 220–235,
 1421 doi:10.1029/2012JD018165, 2013.
 1422
 1423 Vadrevu, K.P., Ellicott, E., Badarinath, K.V.S., Vermote, E.: MODIS derived fire
 1424 characteristics and aerosol optical depth variations during the agricultural residue burning
 1425 season, north India. *Environmental Pollution* 159, 1560–1569, 2011.
 1426
 1427 Vadrevu, K. P., Giglio, L., Justice C.: Satellite based analysis of fire–carbon monoxide
 1428 relationships from forest and agricultural residue burning (2003–2011), *Atmos. Environ.*,
 1429 64, 179–191, 2013.
 1430
 1431 van der Werf, G. R., Randerson, J. T., Giglio, L., Collatz, G. J., Mu, M., Kasibhatla, P. S.,
 1432 Morton, D. C., DeFries, R. S., Jin, Y., and van Leeuwen, T. T.: Global fire emissions and the
 1433 contribution of deforestation, savanna, forest, agricultural, and peat fires (1997–2009),
 1434 *Atmos. Chem. Phys.*, 10, 11707–11735, doi:10.5194/acp-10-11707-2010, 2010.
 1435
 1436 Venkataraman, C., Habib, G., Eiguren-Fernandez, A., Miguel, A. H., and Friedlander, S. K.:
 1437 Residential biofuels in south asia: Carbonaceous aerosol emissions and climate impacts,
 1438 *Science*, 307, 1454–1456, 2005
 1439

Xiaohua 1/14/2015 1:46 PM

Deleted: Tare, V., et al.: Measurements of atmospheric parameters during Indian Space Research Organization Geosphere Biosphere Program Land Campaign II at a typical location in the Ganga Basin: 2. Chemical properties, *J. Geophys. Res.*, 111, D23210, doi:10.1029/2006JD007279, 2006. .

1448 Venkataraman, C., Habib, G., Kadamba, D., Shrivastava, M., Leon, J.-F., Crouzille, B.,
1449 Boucher, O. and Streets, D. G.: Emissions from open biomass burning in India: Integrating
1450 the inventory approach with high-resolution Moderate Resolution Imaging
1451 Spectroradiometer (MODIS) active-fire and land cover data, Global Biogeochem. Cycles, 20,
1452 GB2013, doi:10.1029/2005GB002547, 2006.
1453
1454 Yasunari, T. J., Bonasoni, P., Laj, P., Fujita, K., Vuillermoz, E., Marinoni, A., Cristofanelli, P.,
1455 Duchi, R., Tartari, G., and Lau, K.-M.: Estimated impact of black carbon deposition during
1456 pre-monsoon season from Nepal Climate Observatory – Pyramid data and snow albedo
1457 changes over Himalayan glaciers, Atmos. Chem. Phys., 10, 6603-6615, doi:10.5194/acp-
1458 10-6603-2010, 2010.
1459 |
1460

Xiaohua 1/14/2015 1:47 PM

Deleted: .

... [4]

1463 **Tables**
1464 Table1. General information of multi-models.
1465

Model	ID	Time range	Res. ^a	Anthrop. Emi. ^b	BB Emi. ^c	Met. Field	Extra ^d Species	References
HadGEM2	HAD	2000-2006	1.8×1.2×38	A2-MAP	GFED2	ERA-Interim	NO ₃ ⁻ , SOA	Bellouin et al., 2011
GOCART-v4	GOC	2000-2007	2.5×2×30	A2-MAP	GFED2	GEOS-DAS	-	Chin et al., 2002,2009
ECHAM5-HAMMOZ	ECH	2000-2005	1.8×1.8×31	A2-MAP	GFED2	ECMWF analysis	SOA	Pozzoli et al., 2011
GISS-modelE	GIE	2000-2008	2.5×2×40	A2-ACCMIP	GFED2	NCEP wind,	NO ₃ ⁻ , SOA	Tsigaridis et al., 2013
GISS-MATRIX	GIM	2000-2007	2.5×2×40	A2-ACCMIP	GFED2	NCEP-wind	NO ₃ ⁻	Bauer et al., 2008, 2010
SPRINTARS	SPR	2000-2008	1.1×1.1×56	A2-ACCMIP	GFED2	NCEP/NCAR	-	Takemura et al., 2005,2009
GEOS5-GOCART	GE5	2000-2008	2.5×2×72	A2-ACCMIP	GFED2	MERRA	-	Colarco et al., 2010

^a Spatial resolutions (°latitude x °longitude x number of vertical levels)

^b Anthropogenic emission data are from either A2-ACCMIP or A2-MAP (refer to Diehl et al. 2012)

^c Biomass burning emission data (refer to Diehl et al. 2012)

^d Extra aerosols, either SOA (secondary organic aerosol) or NO₃⁻ (nitrate), besides commonly included aerosol species, i.e. SO₄²⁻ (sulfate), Dust, SS (sea salt), BC (black carbon), and OA(organic aerosol).

1488 Table 2. Summary of stations in South Asia used in this study
1489

Type	Station ^a	Lat	Lon	Alt (m)	Popul- ation ^b (milli-)	Data Source ^c	Data Category	Main Feature
Urban	Delhi	28.58° N	77.20° E	260	16.75	ICARB	BC	In western IGP, the largest city in India
	Karachi	24.87° N	67.03° E	49	13	AERONET	AOD AAOD	Coastal location in southern Pakistan
	Lahore	31.54° N	74.32° E	270	9	AERONET	AOD AAOD	In western IGP, major agricultural region
	Hyderabad	17.48° N	78.40° E	545	6.81	ICARB	BC	In central Indian Peninsula
	Pune	18.52° N	73.85° E	559	5.05	ICARB	BC	In western plateau
	Kanpur	26.51° N	80.23° E	123	2.77	AERONET/ ISRO-GBP	Misc. ^d	In central IGP
	Agra	27.06° N	78.03° E	169	1.75	ISRO-GBP	Misc. ^d	Between Delhi and Kanpur
Semi- Urban	Allahabad	25.45° N	81.85° E	98	1.22	ISRO-GBP	Misc. ^d	In central-eastern IGP
	Kharagpur	22.52° N	87.52° E	28	0.37	ICARB	BC	In eastern IGP-outflow region to Bay of Bengal
	Hisar	29.09° N	75.42° E	41	0.3	ISRO-GBP	Misc. ^d	Surrounded by agricultural field in western IGP
	Trivandrum	8.55° N	76.90° E	3	0.75	ICARB	BC	A coastal station in southern India
Remote	Port Blair	11.63° N	92.70° E	60	0.1	ICARB	BC	Island in Bay of Bengal
	Nainital	29.20° N	79.30° E	1950	0.04	ICARB	BC	High altitude remote location in the Himalayan foothills
	Minicoy	8.30° N	70.00° E	1	0.009	ICARB	BC	Island in Arabian Sea

1490 ^a. In an order of the population

1491 ^b. Statistics in 2011 from wikipedia

1492 ^c. Details in section 3.2 and 3.3

1493 ^d. Miscellaneous, including meteorological fields, AOD, AAOD and aerosol surface
1494 concentration.

1495

1496

1497 **Figures**
 1498 Captions
 1499

1500 Fig. 1. Topography of South Asia overlapped with stations used in this study. Three
 1501 AERONET stations are labeled in blue, eight ICARB stations in red and four ISRO-GBP
 1502 stations in black except Kanpur. Topography map is obtained from
 1503 <http://mapofasia.blogspot.com/2013/02/map-of-south-asia-area-pictures.html>.
 1504

1505 Fig. 2. Spatial distribution of anthropogenic emissions of BC, OA, SO₂, NH₃ and NO_x
 1506 averaged for 2000-2007 from A2-ACCMIP emission dataset (units: g m⁻² yr⁻¹). The annual
 1507 averaged mean emission over South Asia is shown at the upper right corner.
 1508

1509 Fig. 3. Spatial distribution of biomass burning emission of BC based on GFED2 for each
 1510 season averaged for 2000-2007 (units: g C m⁻² yr⁻¹). The seasonal averaged emission
 1511 amount over South Asia is shown at the upper right corner. Note that the color scale is
 1512 consistent with that in the Fig. 2 for BC.
 1513

1514 Fig. 4. The annual averaged mean AOD for 2000-2007 over (a) South Asia (the green area in
 1515 the map); (b) Central IGP (77°-83°E; 25°-28°N, the white box in that map). The thin curves
 1516 with symbols represent seven models, and the thick curves represent four NASA remote
 1517 sensors, with corresponding multi-year averaged annual mean AOD and the standard
 1518 deviation followed.
 1519

1520 Figure 5. Monthly mean AOD (left column) and AAOD (right column) in a two-year period
 1521 over 3 AERONET stations in South Asia. The gray bar represents measurement from
 1522 AERONET. The thin curves represent seven models, and symbols represent three NASA
 1523 remote sensors. On each panel, corr=correlation coefficient of a model with AERONET,
 1524 bias=relative mean bias, i.e. $\Sigma(\text{MODEL}_i)/\Sigma(\text{AERONET}_i)$, rmse=root-mean-square error
 1525 relative to AERONET.
 1526

1527 Fig. 6. AOD of total aerosol (aer) and components (ss, so₄, bc, oa, dust, no₃, soa and bb) at
 1528 Kanpur for 2004 in 4 models, HAD (upper left), SPR (upper right), GES (lower left) and GOC
 1529 (lower right). The gray bar represents measurement from AERONET. The annual mean
 1530 AOD is followed after the name of each symbol. NOTE: bc and oa represent emission from
 1531 fossil fuel only and bb represents emission from biomass burning only).
 1532

1533 Fig. 7a. Spatial distribution of AOD over South Asia in 4 seasons averaged for 2000–2007 in
 1534 three satellite observations (two from MODIS, MISR and SeaWiFS). The corresponding area
 1535 averaged annual mean AOD value is listed in each panel (domain:0–36°N; 55°E–100°E).
 1536 Three AERONET stations used in this study are labeled in the maps. Regions in white
 1537 indicate insufficient sampling sizes of aerosol retrievals due to the presence of bright
 1538 surface or frequent cloud cover in satellite data.
 1539

1540 Fig. 7b. Spatial distribution of AOD over South Asia in 4 seasons averaged for 2000–
 1541 2007 in seven models (the first three models with the anthropogenic emissions from A2-
 1542 MAP and the rest with A2-ACCMIP). The corresponding area averaged annual mean AOD

Xiaohua 1/23/2015 4:19 PM

Deleted: Fig. 5. Monthly mean AOD (left column) and AAOD (right column) in a two-year period over 3 AERONET stations in South Asia. The gray bar represents measurement from AERONET. The thin curves represent seven models, and symbols represent three NASA remote sensors.

1551 value is listed in each panel (domain:0–36°N; 55°E–100°E). Three AERONET stations used
1552 in this study are labeled in the maps.
1553

1554 Fig. 8. The seasonal mean of vertical profile of extinction coefficient (units: 1/km) at (a) Kanpur,
1555 and (b) Hyderabad from CALIOP and seven models. Units of Z_a is km. The corresponding
1556 averaged AOD, Z_a and F_{2km} are listed after each symbol name. The gray shaded area in
1557 CALIOP shows one standard deviation relative to 2006–2011 averages.
1558

1559 Fig. 9. The comparison of seven models against observations at 8 ICARB stations in terms of
1560 monthly surface BC concentration during 2006 (units: $\mu\text{g m}^{-3}$).
1561

1562 Fig.10. Comparisons of seven models against ISRO-GBP campaign measurements at 4 IGP
1563 stations (Hisar, Agra, Kanpur, Allahabad from west to east) in December 2004. The variables
1564 include two meteorological fields, surface relative humidity (1st row) and surface temperature
1565 (2nd row), four surface mass concentrations, SO_4^{2-} (3rd row), NO_3^- (4th row) with 4 models (GOC,
1566 ECH, SPR, GE5) missing this aerosol module, BC (5th row), and OA (6th row), and two
1567 columnar quantities, AOD (7th row) and AAOD (8th row) at 550nm.
1568

1569 Fig. 11. The mass extinction efficiency at 550nm for individual aerosol components (units:
1570 m^2/g) as a function of relative humidity used by the models GEOS5 and GOCART.
1571
1572
1573
1574
1575
1576
1577
1578

Xiaohua 1/13/2015 5:34 PM

Comment [3]: The caption is changed compared to the one in ACPD

Xiaohua 1/13/2015 5:33 PM

Deleted: Fig.7a. Spatial distribution of AOD over South Asia in winter (DJF) averaged for 2000–2007 from three Satellite observations (the first row) and seven models (in the second row are 3 models with the anthropogenic emissions from A2-MAP and the rest are 4 models with A2-ACCMIP). The corresponding area averaged annual mean AOD is listed in each panel (domain: 0–36°N; 55°E–100°E). Three AERONET stations used in this study are labeled in the maps. Regions in white indicate insufficient sampling sizes of aerosol retrievals due to the presence of bright surface or frequent cloud cover in satellite data.

Fig. 8. The seasonal variation of vertical vertical profile of extinction coefficient (units: 1/km) at (a) Kanpur, and (b) Hyderabad. Units of Z_a is km. The corresponding averaged AOD, Z_a and F_{2km} are listed after each symbol name.

Xiaohua 1/13/2015 5:34 PM

Deleted: Fig. 8. The seasonal variation of vertical profile of extinction coefficient (units: 1/km) at (a) Kanpur, and (b) Hyderabad. Units of Z_a is km. The corresponding averaged AOD, Z_a and F_{2km} are listed after each symbol name.

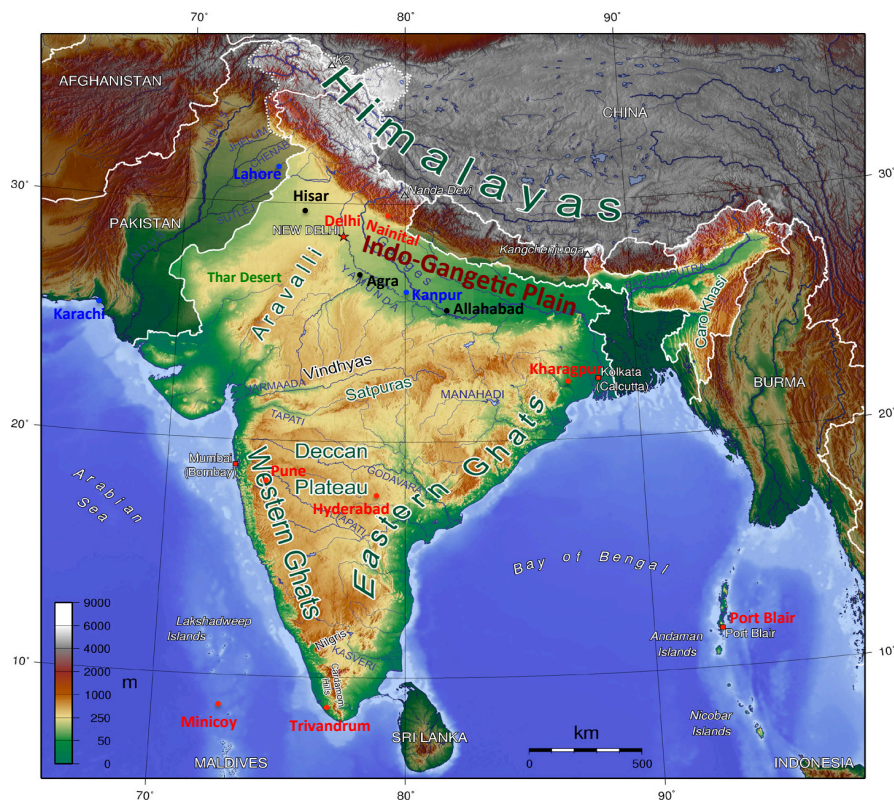
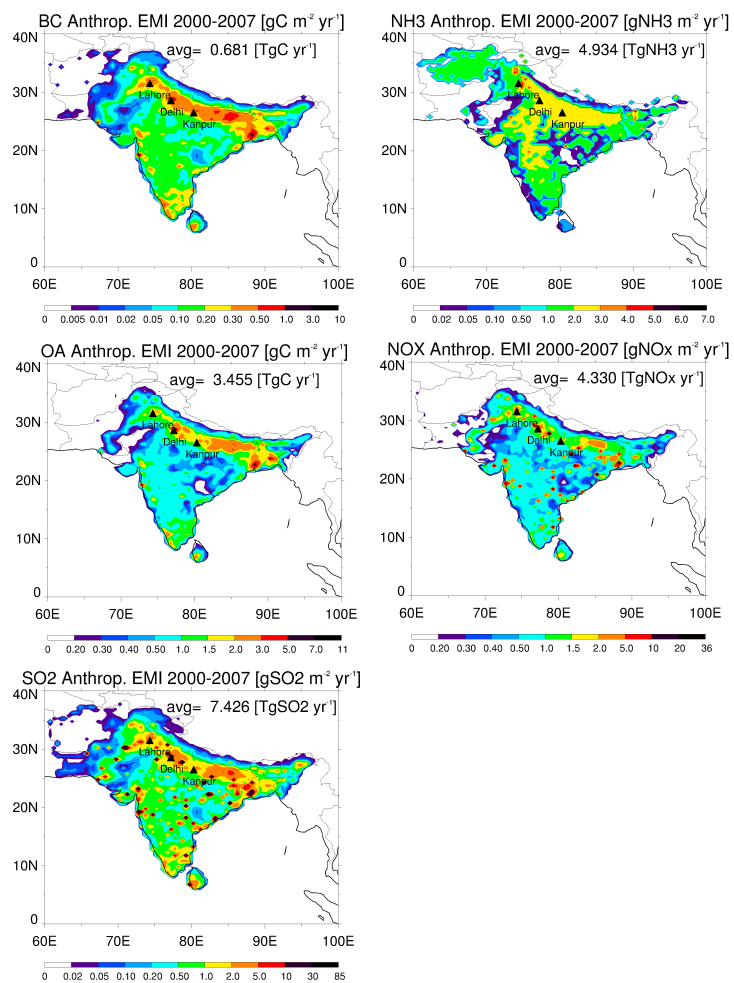


Fig. 1.



1609 Fig. 2.

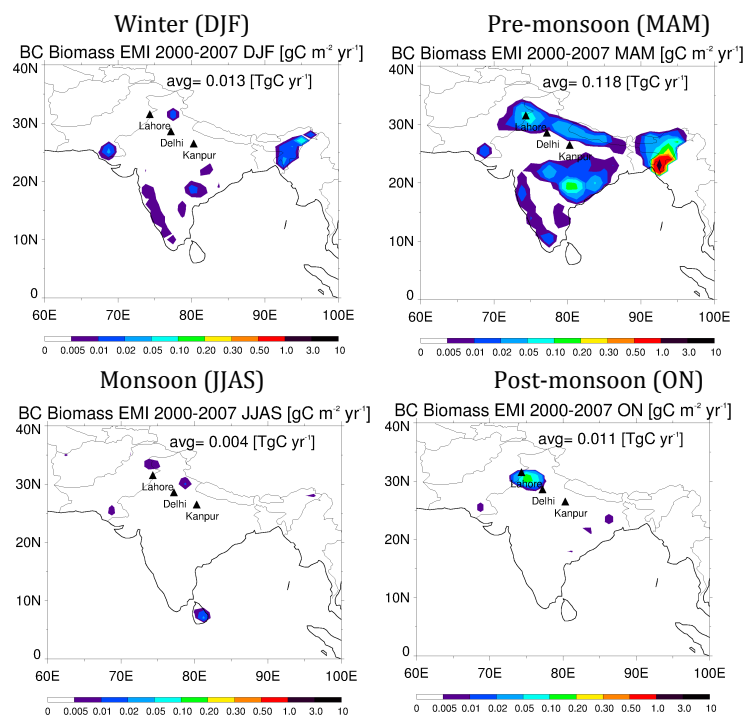
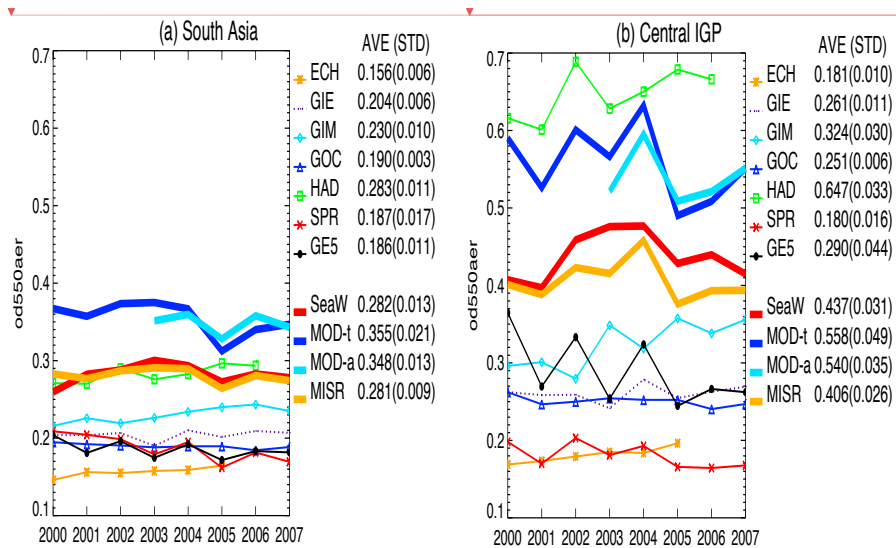


Fig. 3.

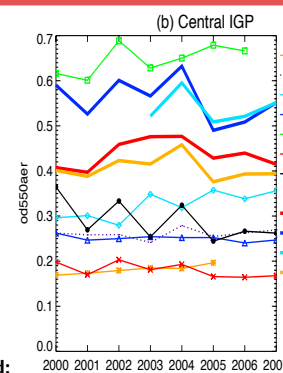
Annual mean AOD (2000-2007)



Xiaohua 1/13/2015 5:35 PM

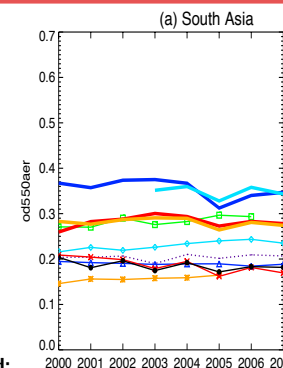
Deleted: <sp>

Xiaohua 1/13/2015 5:35 PM



Deleted:

Xiaohua 1/13/2015 5:35 PM



Deleted:

1620 Fig. 4.
1621

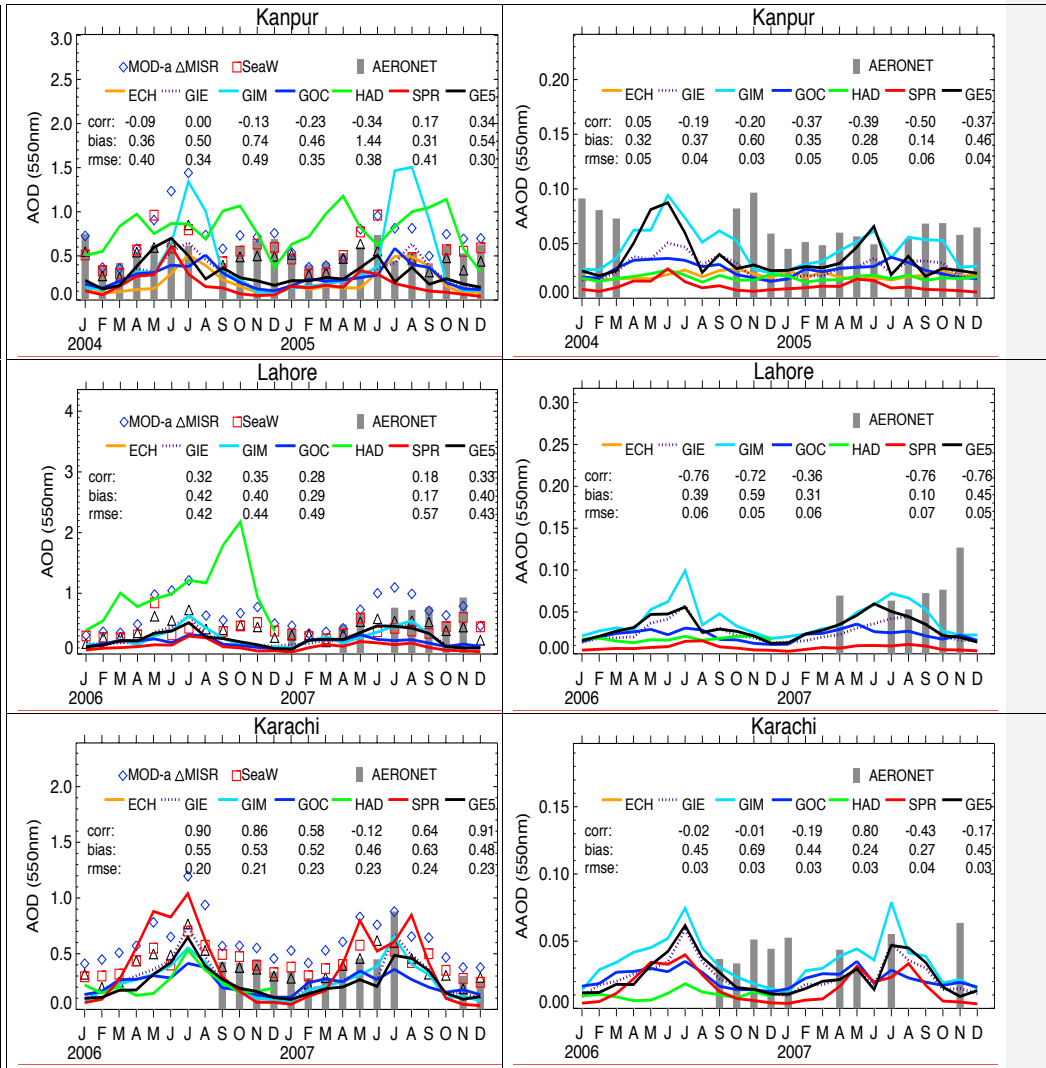


Fig. 5.

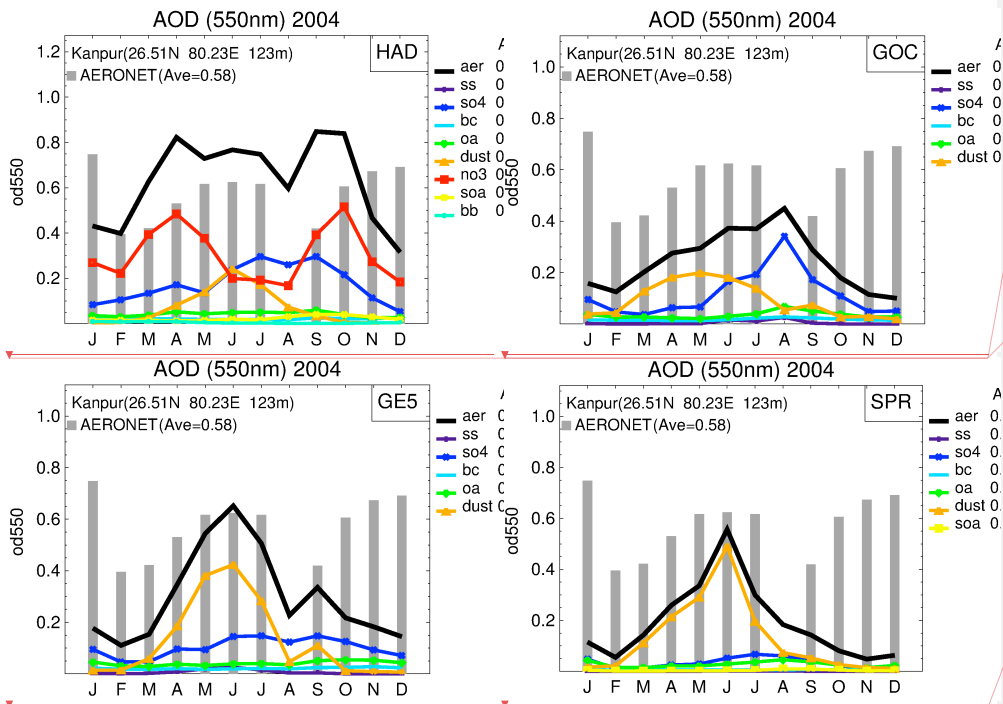
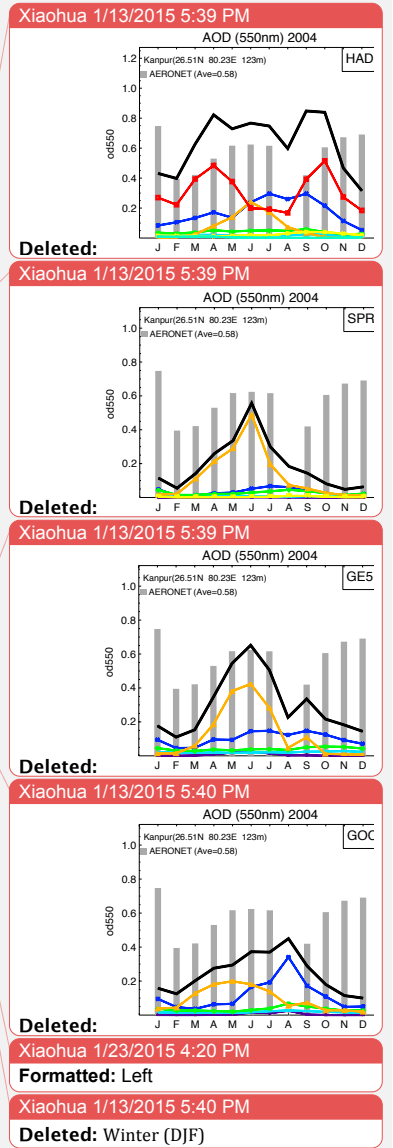


Fig. 6.



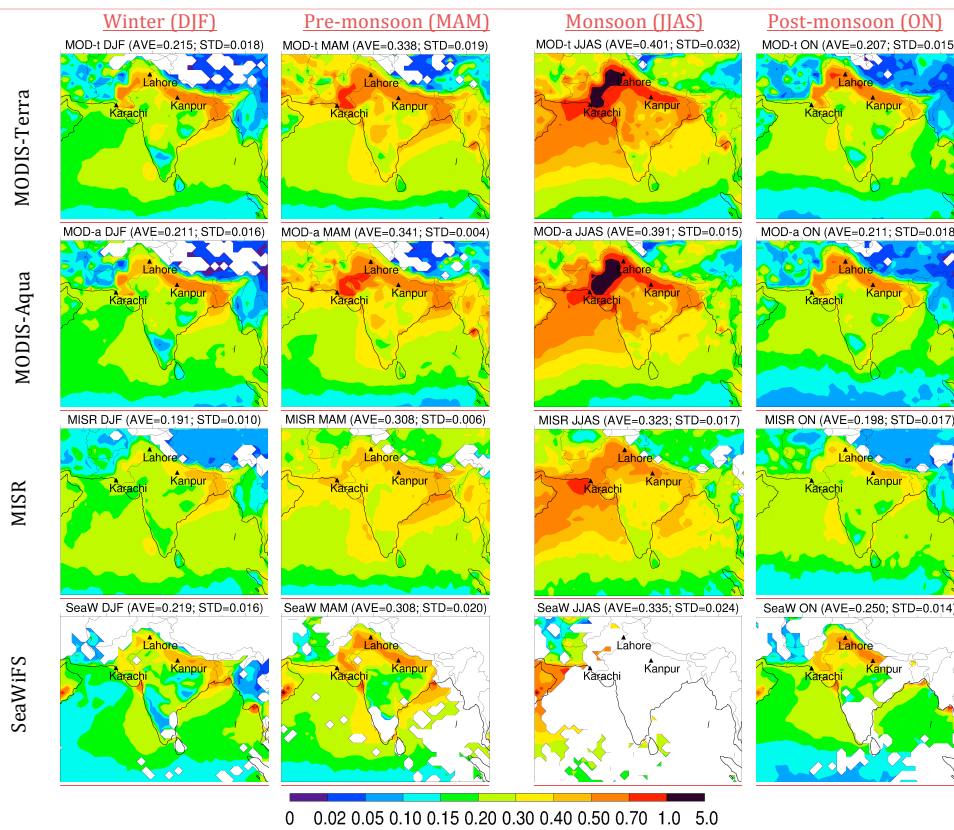
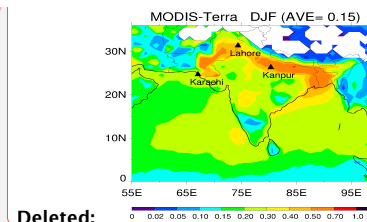
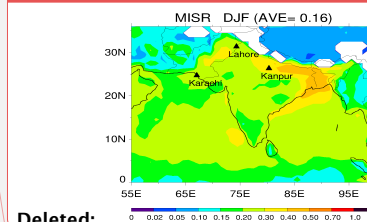


Fig. 7a



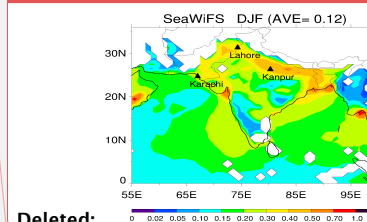
Deleted:

Xiaohua 1/13/2015 5:40 PM



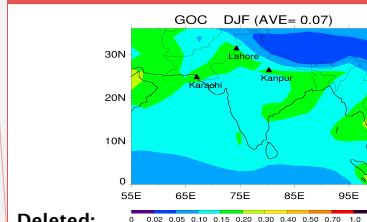
Deleted:

Xiaohua 1/13/2015 5:40 PM



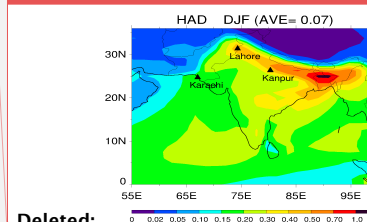
Deleted:

Xiaohua 1/13/2015 5:40 PM



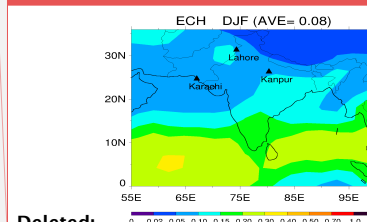
Deleted:

Xiaohua 1/13/2015 5:40 PM



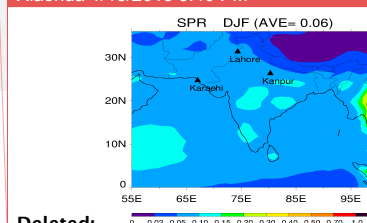
Deleted:

Xiaohua 1/13/2015 5:40 PM



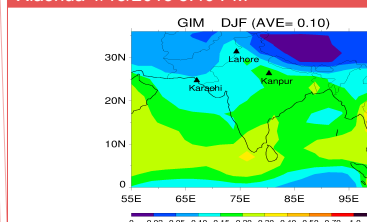
Deleted:

Xiaohua 1/13/2015 5:40 PM



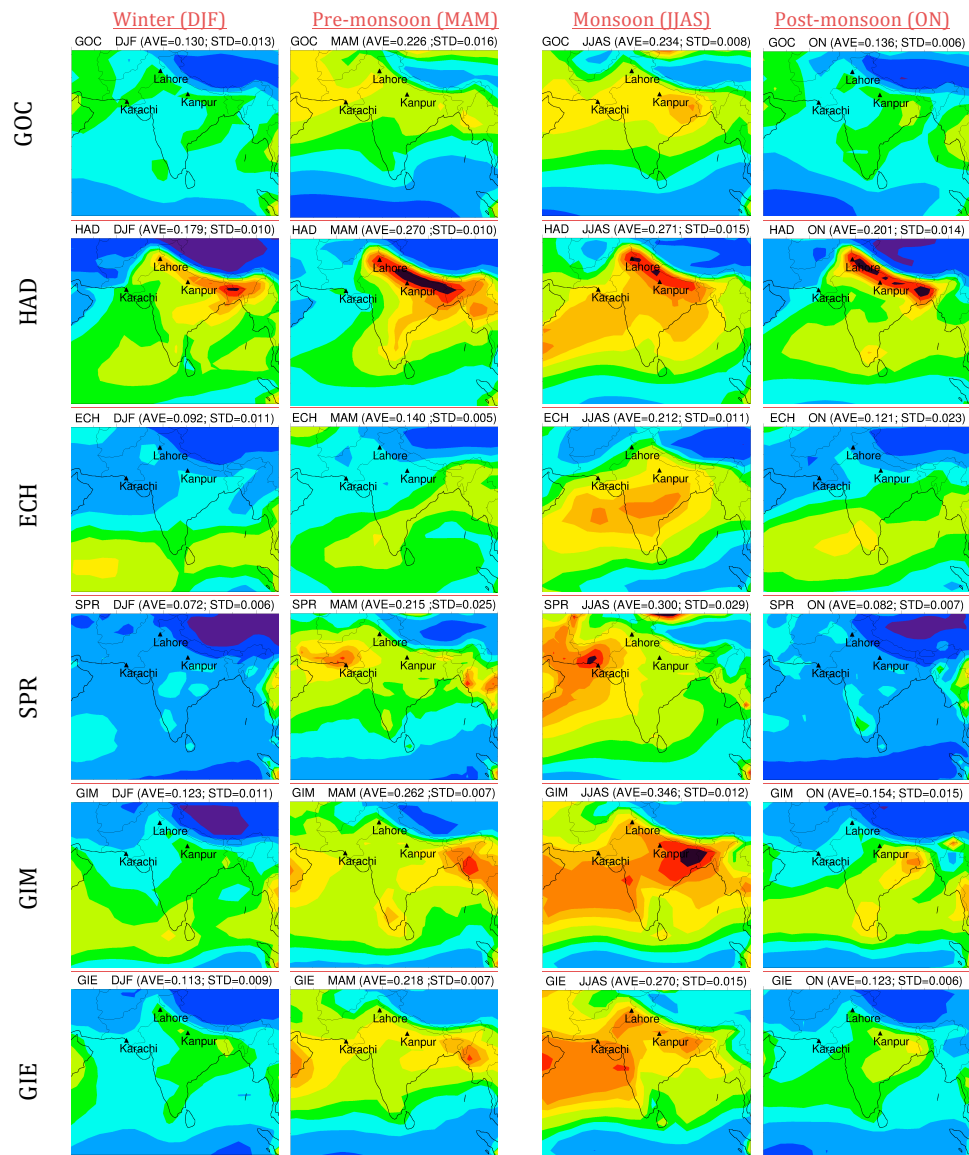
Deleted:

Xiaohua 1/13/2015 5:40 PM



Deleted:

Xiaohua 1/13/2015 5:40 PM



GE5

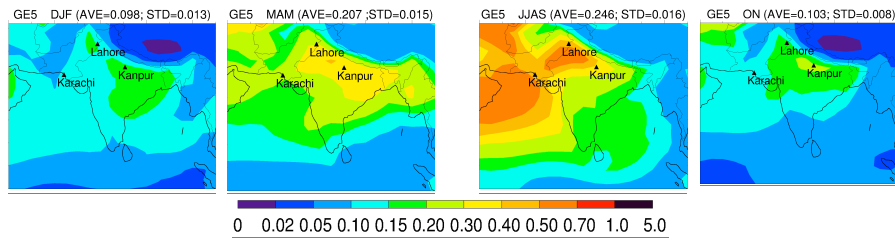
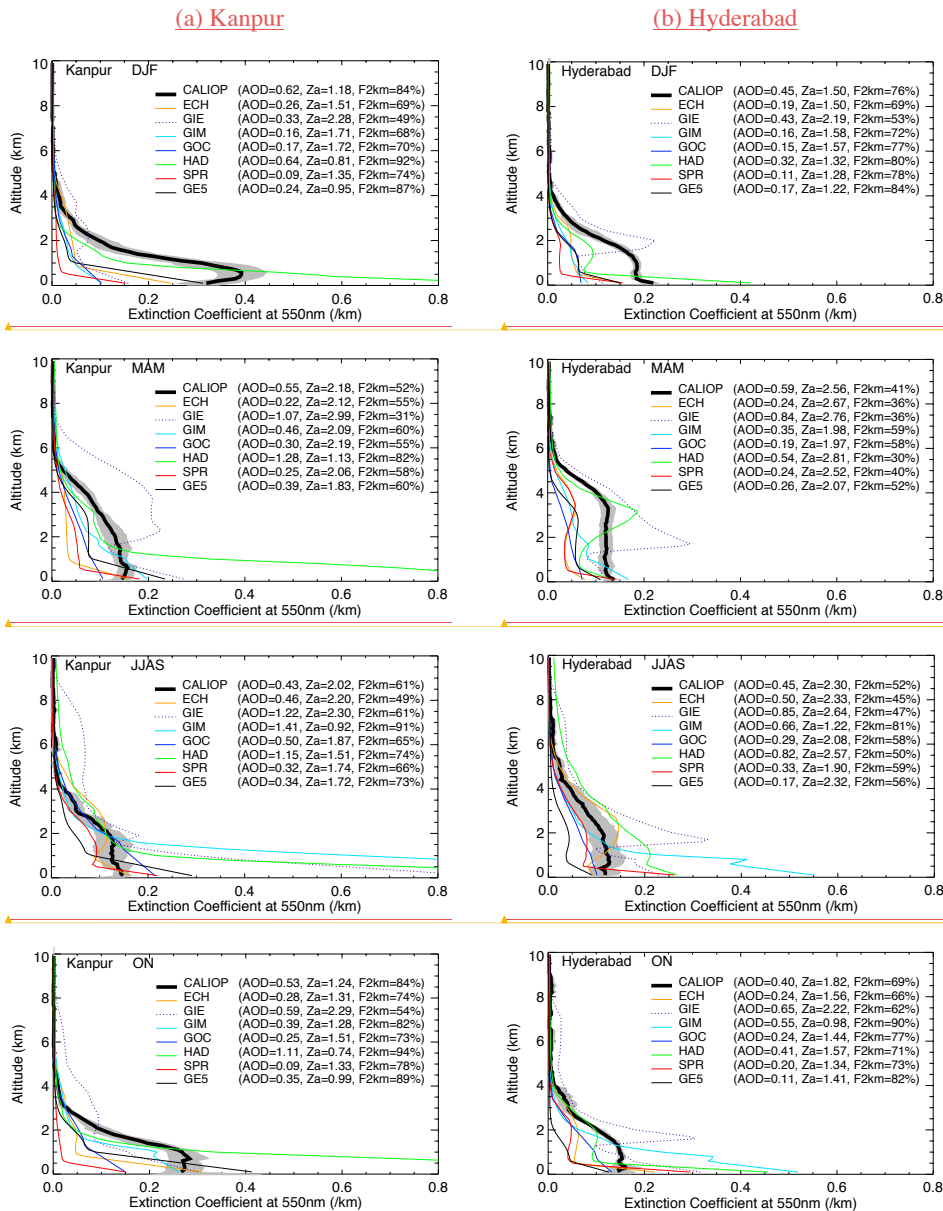


Fig. 7b.



Unknown
Formatted: Font:(Default) Times

Unknown
Formatted: Font:(Default) Times

Unknown
Formatted: Font:(Default) Times

Unknown
Formatted: Font:(Default) Times

Unknown
Formatted: Font:(Default) Times

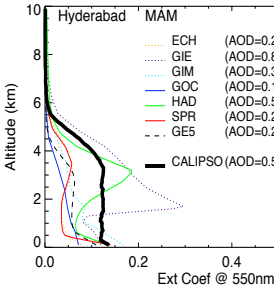
Unknown
Formatted: Font:(Default) Times

Unknown
Formatted: Font:(Default) Times

Unknown
Formatted: Font:(Default) Times

Xiaohua 1/13/2015 6:03 PM
Formatted: Left

Xiaohua 1/13/2015 5:54 PM
Deleted: Fig. 7b.



Deleted:

Xiaohua 1/13/2015 6:02 PM

Formatted Table

Unknown

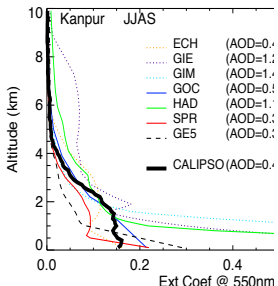
Formatted ... [6]

Unknown

Formatted: Font:Times New Roman, 9 pt

Unknown

Formatted: Font:Times New Roman, 9 pt



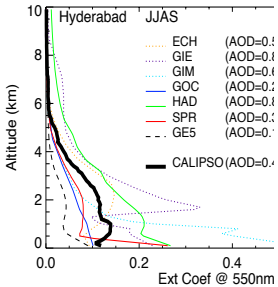
Deleted:

Xiaohua 1/13/2015 6:04 PM

Formatted: Font:Times New Roman, 9 pt

Unknown

Formatted: Font:Times New Roman, 9 pt



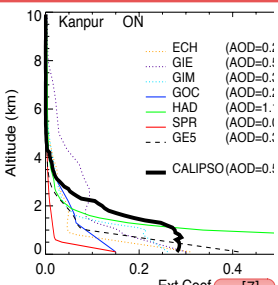
Deleted:

Unknown

Formatted: Font:Times New Roman, 9 pt

Unknown

Formatted: Font:Times New Roman, 9 pt



Deleted:

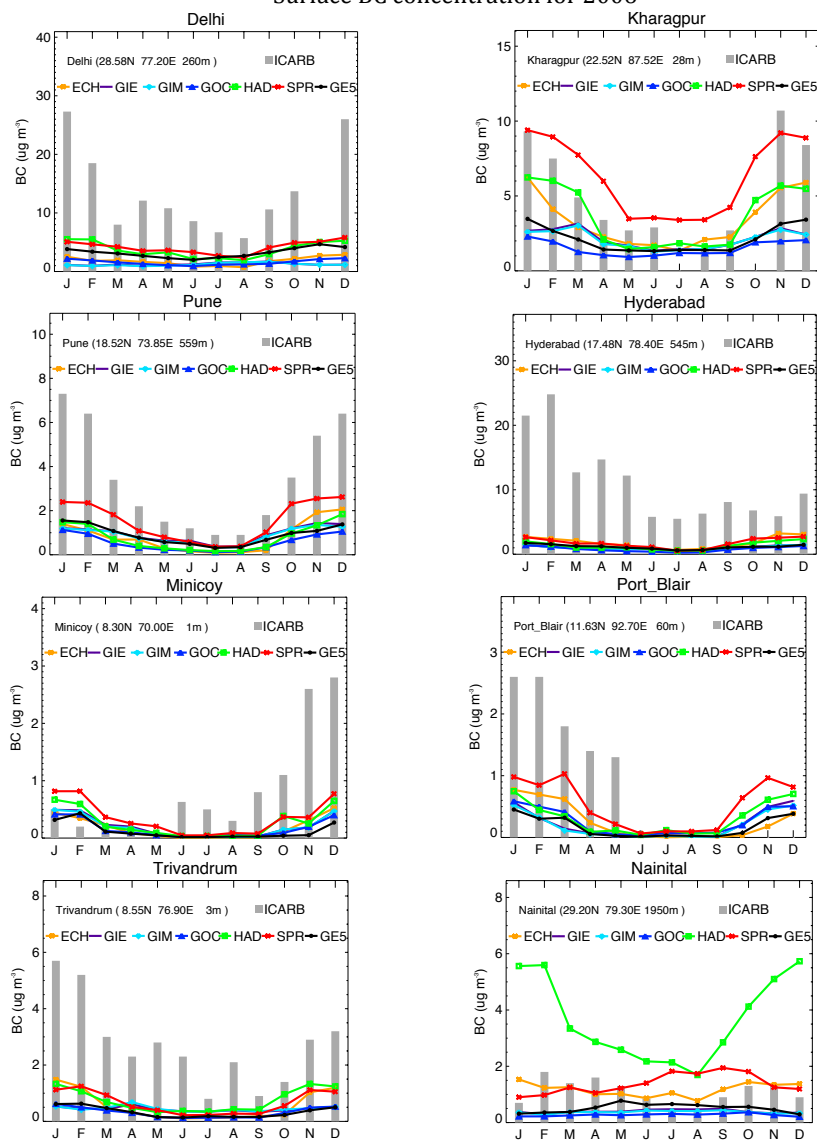
Unknown

Formatted ... [7]

Formatted ... [8]

1678
1679

Surface BC concentration for 2006



1680
1681 Fig. 9.
1682

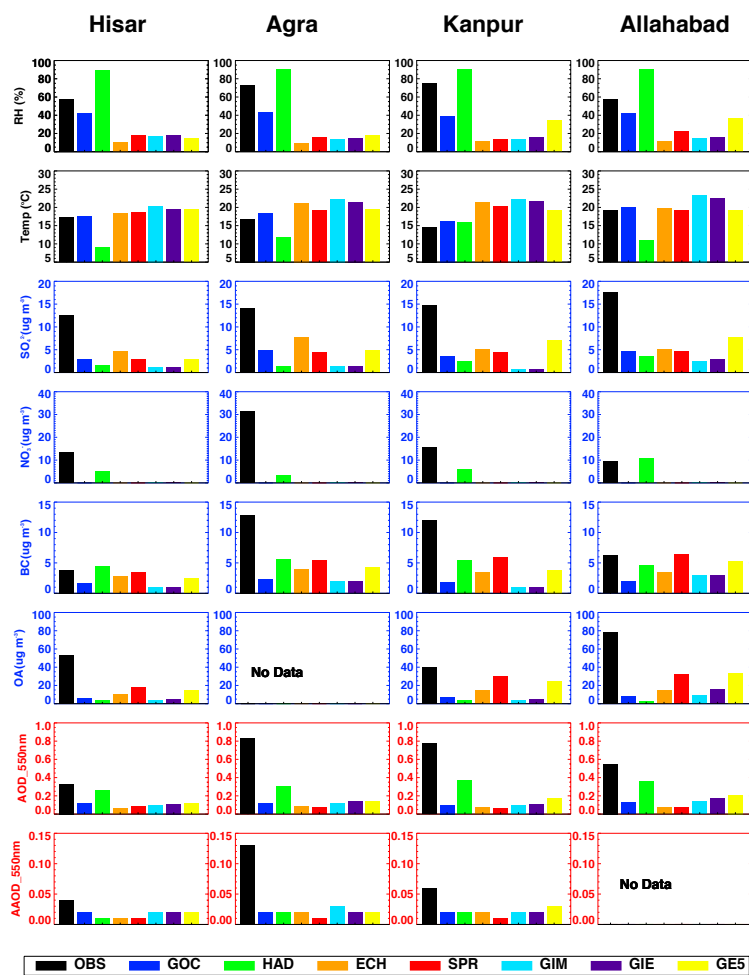


Fig.10.

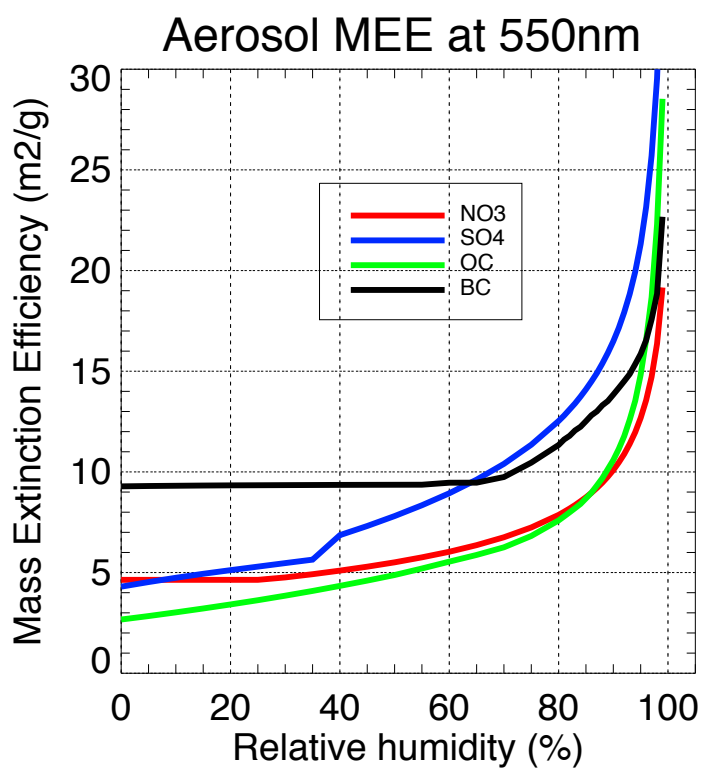


Fig. 11.